Methanol/ Ethanol/ Butanol-Gasoline Blends Use in Transportation Engine-Part 1: Combustion, Emissions, and Performance Study

Akhilendra Pratap Singh, Utkarsha Sonawane, Avinash Kumar Agarwal*

Engine Research Laboratory, Department of Mechanical Engineering

Indian Institute of Technology Kanpur, Kanpur-208016, India

*Corresponding Author's email: akag@iitk.ac.in

Abstract

Primary alcohols such as methanol, ethanol, and butanol have exhibited excellent potential as possible alternative fuels for spark ignition (SI) engines because they are renewable, cleaner and safer to store and transport. However, it remains important to investigate the technical feasibility of adapting these primary alcohols in existing SI engines. In this research, a multi-point port fuel injection (MPFI) system equipped SI engine was used for assessing and comparing the combustion, performance, and emission characteristics of various alcohol-gasoline blends (gasohols) vis-à-vis baseline gasoline. The experiments were performed for different engine loads at rated engine speed. Experimental results exhibited relatively superior combustion characteristics of the engine fueled with gasohol than the baseline gasoline, especially at medium engine loads. Among different test fuels, the methanol-gasoline blend (GM10) exhibited relatively more stable combustion characteristics than the ethanol-gasoline blend (GE10) and butanol-gasoline blend (GB10). In this study, relatively superior engine performance of the gasohol-fueled engine was observed at all engine loads and speeds. GB10 exhibited the highest brake thermal efficiency (BTE), followed by GM10 amongst all test fuels. The

effect of improved combustion was also reflected in the emission characteristics, which exhibited that GB10 emitted relatively lower carbon monoxide (CO) and hydrocarbons (HC) than other test fuels. GB10 emitted relatively higher nitrogen oxides (NOx) than GM10 and GE10. Unregulated emission results exhibited that the engine fueled with gasohols emitted relatively lower sulfur dioxide (SO_2), ammonia (NH_3), and various saturated and unsaturated HCs than the baseline gasoline. The GM10-fuelled engine was relatively more effective in reducing unregulated emissions among all test fuels. This study concluded that methanol and butanol blending with gasoline resulted in superior engine performance and reduced harmful emissions in MPFI transport engines. This offered an excellent option to displace fossil fuels partially and reduce emissions simultaneously.

Keywords: Gasohol, Performance, Combustion, Unregulated Emissions, Spark Ignition Engine.

1. Introduction

Increasing demand for crude oil and deteriorating air quality has become the biggest global challenges in the 21st century. Limited resources of fossil fuels and growing energy demand call for exploration of newer non-fossil alternatives for powering internal combustion (IC) engines in various sectors of the economy. As per an estimate, oil, natural gas, and coal reserves will last for 41 years, 63 years, and 218 years respectively [1]. Depleting fossil fuel reserves are responsible for continuously increasing petroleum prices and greenhouse gaseous (GHG) emissions. Market necessity and emission restrictions promoted viable techniques to reduce emissions without compromising engine performance. Refinements in the engine designs, fuel pre-conditioning, alternative fuels, and exhaust gas after-treatment systems were explored to reduce the emissions from IC engines [2]. The catalytic converter was the most widely adopted technique to control engine emissions [3]. However, catalytic converters have several limitations, such as poor efficiency in cold-start conditions and a long time required to activate the catalytic reactions for emission reduction. Several researchers proposed using alternative fuels in IC engines can reduce emissions and dependence on fossil fuels [4] [5]. Many alternative fuels, such as biogas, bio-alcohols, biodiesel, have been extensively investigated. These alternative fuels can be easily adapted in existing IC engines with some minor hardware/ software modifications.

Primary alcohols exhibited significant potential for SI engines to partially displace gasoline [6]. Alcohols are reasonably low-priced and favourable fuels due to vast feedstock availability, safe storage, and easy transportation. Primary alcohols can be produced from agriculture residues, household waste, municipal solid waste, etc., e.g., methanol can be produced from coal, biomass [7], coke oven gas, natural gas [8], and hydrogen. The other advantages of methanol are its wider lean ignition limits and higher octane rating, making it a superior fuel for SI engines than gasoline [9]. Zhen and Wang [10] described methanol production methods systematically and its potential as a renewable fuel. They summarised 13 methanol applications in IC engines and provided suggestions on the weaknesses in the methanol engine research studies. Ethanol is primarily produced from biomass. Its important physical characteristics, such as fuel density and research octane number, make it appropriate for SI engines [11]. Ethanol reduces greenhouse gas (GHG) emissions. Studies have shown that ethanol-gasoline blends (gasohols) reduce carbon monoxide (CO) and hydrocarbon (HC) emissions drastically by promoting complete combustion [12] [11]. Butanol is another primary alcohol, having significant potential for use in SI engines. Relatively higher heating value, higher research octane number, and lower moisture affinity of butanol than other primary alcohols make it suitable as a SI engine fuel. Butanol has physical properties quite close to gasoline, leading to the higher thermal efficiency of butanol-gasoline blends [13]. However, butanol has lower oxygen content than methanol and ethanol, affecting fuel's knock resistance. Higher oxygen content in the test blend offers higher knock resistance. At higher blending ratios, butanol exhibits higher knocking than other primary alcohols. Butanol's relatively higher reactivity and boiling point render it less preferred for SI engines [14]. Zhen et al. [15] introduced butanol in CI and SI engines and explored butanol-fueled engines' future research and development.

Many studies have demonstrated that gasohols resolve the issues of higher NOx and particulate matter (PM) emissions and incomplete combustion faced by SI engines due to their fuel-bound oxygen [16] [17] [18]. In another experimental study [19], alcohol-gasoline blends impressively reduced regulated emissions of CO and HC by ~40% to 50%, respectively. In contrast, gasohols emitted higher unregulated emissions than baseline gasoline [19]. Experiments revealed that gasohol was a cost-effective and efficient alternative to reduce GHG emissions from the engines [20] [21]. SI engines fueled with gasohol exhibited reduced unregulated emissions without significant change in combustion characteristics [22]. However, primary alcohols, especially methanol, may corrode vital components of the fuel injection equipment (FIE) and other metallic engine components, limiting alcohol usage in IC engines. A moderate blending of methanol with gasoline improves combustion due to improved fuel evaporation characteristics. Abu-Zaid [23] investigated the effect of various methanol-gasoline blends on SI engine performance. They concluded that blends with 15% (v/v) methanol show improved engine performance for power output and brake specific fuel consumption (BSFC). However, there are studies on higher blending ratios of methanol in gasoline. M85 (85% methanol and 15% gasoline v/v) usage led to 25% and 80% reductions in CO and NOx emissions, respectively, vis-à-vis baseline gasoline. While, in a few studies, a slightly higher BSFC for methanol-gasoline fueled engines was reported [24] [25]. Prasad et al. [26] investigated methanol-gasoline blend fueled SI engine's performance, combustion, and emission characteristics by varying the compression ratio (CR) to 8, 9, and 10. They reported that methanol-gasoline fueled engines exhibited superior engine performance at higher CRs without knocking. Yucesu et al. [27] performed experiments on a single-cylinder SI engine fueled with ethanol-gasoline blends and reported significant reductions in regulated emissions. Similar studies [27] [28] on ethanol-gasoline-fueled SI engines also exhibited a major reduction in CO and HC emissions. Carbon dioxide (CO_2) emission was reduced due to the leaning effect of ethanol addition (fuel oxygen), whereas NOx emissions didn't correlate with the ethanol proportion in the test fuel. Introduction of 5-10-20-30% (v/v) ethanol in gasoline reduced CO and particulate number emissions, while the volatile organic compounds (VOCs) were not affected [28]. Researchers also explored alcohol blending of gasoline on unregulated emissions from SI engines [29]. Baseline gasoline-fueled engines produced higher unregulated emissions than gasohol fueled engines [30]. Bielaczyc et al. [11] studied the influence of physicochemical attributes on tailpipe emissions of light-duty SI engines fuelled with ethanol-gasoline blends. Unregulated emissions such as ethylene, carbonyl compounds, alcohols, acetaldehyde, and formaldehyde marginally increased due to ethanol blending with gasoline [31]. Poulopoulos et al. [32] reported higher acetaldehyde emissions from ethanol-gasoline blend fuelled engines; however, these emissions were reduced to negligible levels by a catalytic converter. However, the catalytic converter could not reduce ethanol, acetic acid, and hexane emissions. Unregulated emissions like ethanol and acetaldehyde increased with increasing ethanol fraction in the fuel and reduced with increasing engine speed/torque. Formaldehyde emissions increased significantly with increasing engine speed [33]. Gomez et al. [34] performed experiments on a single-cylinder port-injected engine fuelled with methanol-gasoline, ethanol-gasoline, and butanol-gasoline blends (20% v/v). They suggested using primary alcohols for the SI engine to allow a higher compression ratio, hence higher efficiency. The introduction of primary alcohols is a promising way to eliminate knocking in SI engines while allowing higher compression ratios. Kalwar et al. [35] utilised primary alcohols (methanol, ethanol, butanol) in the dual-fuel gasoline direct injection (GDI) engine. They reported that port injection of primary alcohols reduced CO, PM, and NO_x emissions, whereas HC emissions increased slightly from the baseline gasoline. The port induction of alcohols improved the engine combustion and performance characteristics.

The literature review exhibits plenty of research has been done to adapt different gasohols in SI engines. However, most studies focused on combustion, performance, and emission (mostly regulated) characteristics of a specific alcohol-gasoline blend in new-generation engines. Very few studies are available in the literature that compares the combustion, performance, and emission characteristics of existing vehicles fuelled with different alcohol-gasoline blends. Therefore, in this study, experiments were conducted on a medium-duty SI engine fuelled with different alcohol-gasoline blends, namely GM10 (10% methanol and 90% gasoline on a volume basis), GE10 (10% ethanol and 90% gasoline on a volume basis), and GB10 (10% butanol and 90% gasoline on a volume basis) vis-à-vis baseline gasoline to compare the engine combustion, performance, regulated and unregulated emissions characteristics. The objective of this study was to explore the utilisation potential of different primary alcohols in existing SI engines of contemporary port fuel injection (PFI) engine technology used in the transport sector worldwide. Experiments were performed at different engine torques (0, 10, 20, 30, 40, and 50 Nm) at a constant engine speed of 2500 rpm (rated speed). All other variables, such as coolant temperature, intake air temperature, etc., were maintained constant during the experiment. Feasibility analysis of alcohol-gasoline blends based on combustion, performance, and emission characteristics is a novel aspect of this study. Another novel aspect of this experimental study was comparing the unregulated emission species and their relationship with combustion and performance characteristics of the engine fuelled with GM10, GE10, and GB10 vis-à-vis baseline gasoline. The detailed particulate characterisation was also carried out and reported in the second part of this study to explore the suitability of different alcohols in SI engines.

2. Experimental Setup and Methodology

In this study, experiments were conducted using a medium-duty, multi-point port fuel injection (MPFI) automotive engine (Maruti Suzuki; Zen). Figure 1 shows the schematic of the experimental setup.

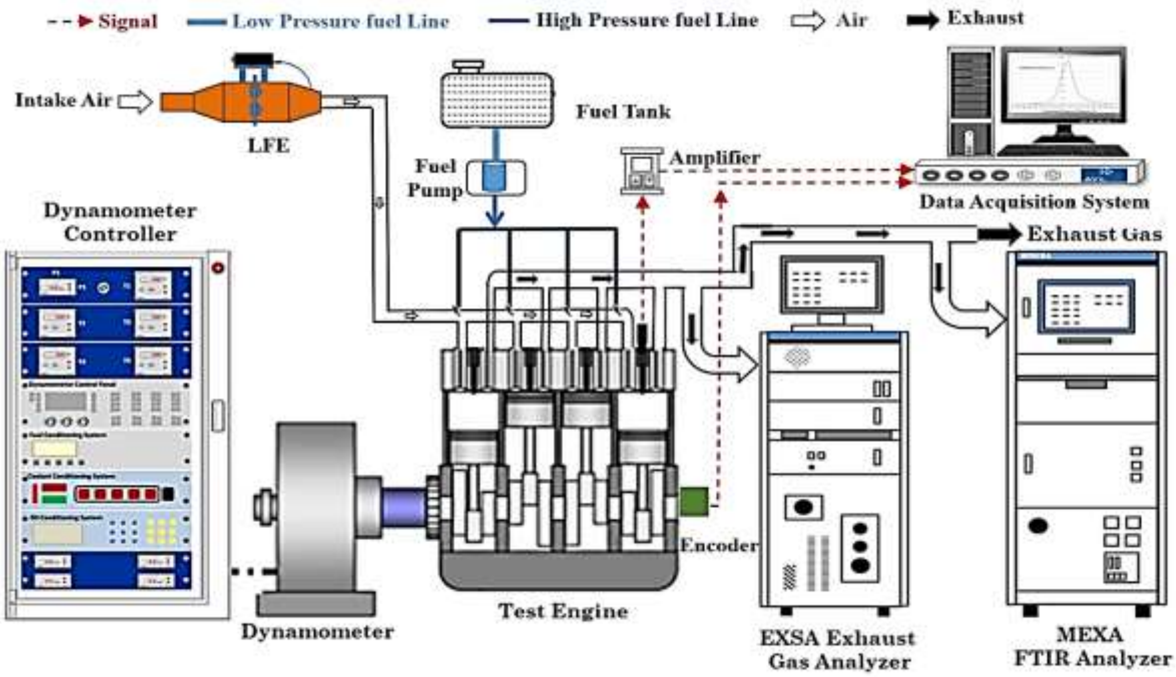

Figure 1: Schematic of the experimental setup

The engine test cell was equipped with several sub-systems: e.g. fuel flow-rate measurement system, combustion data acquisition system, emission measurement system, FTIR emission analyser, temperature measurement system, etc. An eddy current dynamometer (Dynalec; ECB50-200) and a dynamometer controller were used to load the engine and control the engine speed. Important technical specifications of the test engine and dynamometer are given in Table 1.

Table 1: Technical specifications of the test engine and the dynamometer

Test Engine	
Make/ Model	Maruti Suzuki/ Zen
No. of Cylinders	4

Engine displacement	993 cm^3
Bore/ Stroke	72/ 61 mm
Rated Load	71 Nm @ 4500 rpm
Rated power	40 PS @ 6500 rpm
Compression ratio	8.8
Eddy Current Dynamometer	
Make/ Model	Dynalec Controls/ ECB-50-200
Maximum Torque	235 Nm @ 1500-3500 rpm
Maximum Power	120 HP @ 3500-10000 rpm
Uncertainty in torque	±1 Nm

A U-tube manometer was installed across the laminar flow element (LFE) to measure the intake air-flow rate. LFE addresses issues related to pulsating and turbulent flows. Test fuel was injected into the engine's intake port using a low-pressure fuel injection system at 3 bar fuel injection pressure (FIP). This fuel injection system uses several components: a fuel tank, a fuel filter, an electric low-pressure fuel pump, a fuel rail, and a solenoid port fuel injector. Signals for controlling the fuel injection and spark timing were given by an electronic control unit (ECU). Combustion analysis was carried out using the in-cylinder pressure-crank angle data, measured using a piezoelectric pressure transducer (AVL; GH13Z-24). A special spark-plug adaptor was used for housing the pressure transducer in the engine cylinder head. Charge signals produced by the piezoelectric pressure transducer were conditioned by the charge amplifier (AVL; 3066A02). In this charge amplifier, low magnitude charge signals were converted into proportional voltage signals and then amplified to a range of 0-5 V before acquisition by the high-speed combustion analyser (AVL; 619 indimeter). A high-precision shaft encoder (AVL; 365CC) measured the engine crankshaft rotation with high precision.

All signals were given to the high-speed combustion analyser, where software (AVL; INDIWIN-2.2) was used to analyse and calculate combustion-related parameters. The exhaust gas temperature (EGT) was measured using a K-type thermocouple mounted in the exhaust manifold and displayed on a temperature indicator (Pedigree; DTI 4001T). For measuring regulated emissions of HC, CO, and NOx, a raw exhaust gas emission analyser (Horiba; EXSA-1500) was used. Exhaust gas was supplied via a heated exhaust sampling line, maintained at 191°C, to eliminate condensation of moisture and HCs during the sample transport via the pipeline from the engine to the analyser. CO and CO_2 emissions were measured by a non-dispersive infrared (NDIR) analyser. Total hydrocarbons (THC) measurements were done by a hot Flame Ionization Detector (HFID), which could measure a high concentration of HCs with great precision. A chemiluminescence analyser (CLD) was used to measure the engine exhaust's NOx emissions. Raw exhaust gas emission analyser had a wide range of measurements for regulated emissions: 0-5000 ppm for CO; 0-20 vol% for CO_2; 0-5000 ppm for NO/NOx; and 0-50000 ppm for THC. A Fourier transform infrared (FTIR) emission analyser (Horiba; MEXA-6000FT-E) was used to measure the unregulated emissions in the exhaust. This analyser could simultaneously determine 31 different unregulated emissions concentrations using a 'multivariate analysis algorithm.' Experiments were performed using four test fuels, namely GM10, GE10, GB10, and baseline gasoline. All alcohol-gasoline blends were prepared in the laboratory and kept for 48 h to ensure no phase separation and chemical reactions. Important fuel properties of gasoline-alcohol blends and baseline gasoline were measured and shown in Table 2.

Table 2: Important test fuel properties

	G100	GM10	GE10	GB10
Fuel Composition	Gasoline	10% v/v Methanol blended with 90% Gasoline	10% v/v Ethanol blended with 90% Gasoline	10% v/v Butanol blended with 90% Gasoline
Lower Calorific value (MJ/kg)	43.76	40.09	41.18	41.83
Viscosity (mm^2/s) @ 40° C	0.44	0.48	0.54	0.62
Density (g/cm^3) @ 30° C	0.738	0.742	0.751	0.758
Oxygen content (% w/w)	0	5.49	3.71	2.47

* Values available in the literature

The experiments were conducted for G100, GM10, GE10, and GB10 at various engine loads and speeds. Experiments were conducted at six engine loads from 10 to 50 Nm in the steps of 10 Nm at a constant engine speed of 2500 rpm. Also, experiments were performed at different engine speeds from 1500 to 3500 rpm in steps of 1000 rpm at a constant torque of 30 Nm. The results of the engine speed variations are presented and discussed comprehensively in the supporting information section. The objective of this study was to compare the performance, combustion, and emission characteristics of all test fuels. More emphasis has been given to unregulated emissions. Important details of the experimental conditions and experimental methodology are shown in figure 2.

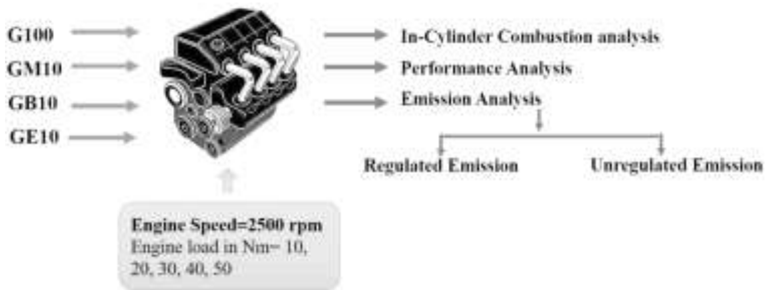

Figure 2: Experimental methodology

3. Results and Discussion

The results and discussion are divided into four sub-sections, covering (i) combustion characteristics, (ii) performance characteristics, (iii) regulated emissions, and (iv) unregulated emissions. In each sub-section, results are discussed to present the effect of engine load on engine combustion, performance, and emissions. The influence of engine speed was insignificant on these parameters; therefore, the effect of engine speed is included in the Supporting Information. Measurements were taken after the thermal stabilisation of the engine to reduce the experimental errors. All experiments were repeated thrice, and the root-of-the-sum-of-the-squares method was adapted for the uncertainty analysis of the experimental data.

3.1 Combustion Characteristics

In this study, combustion characteristics of the SI engine fueled with gasohol vis-à-vis baseline gasoline were assessed at various loads. All combustion characteristics were assessed at a constant engine speed of 2500 rpm. Combustion characteristics included in-cylinder pressure analysis, heat release rate (HRR) analysis, and combustion timings such as the start of combustion (SoC), combustion phasing (CP), and combustion duration (CD). Figure 3(a) shows the in-cylinder pressure variations of gasohols (GM10, GE10, GB10) and baseline gasoline-fueled engines at varying engine loads. The effect of engine speed on variations in the cylinder pressure and HRR is included in the Supporting information (figure S1). Cylinder pressure is greatly influenced by combustion efficiency, which is affected by the rate of fuel-air mixing. Increasing engine load resulted in higher maximum in-cylinder pressure (Pmax) for all test fuels since a higher fuel quantity was injected in every engine thermodynamic cycle to meet the power demand (Figure 3a). The higher fuel quantity burnt resulted in a higher peak in-cylinder pressure and temperature. Relatively superior combustion of alcohol-gasoline blends than baseline gasoline was a major finding. This could be due to the availability of fuel-bound oxygen in alcohol molecules, leading to complete combustion. This was also visible in P_{max} trends, which exhibited relatively higher P_{max} for gasohols than baseline gasoline. However, such an effect was not noticeable at lower loads because of the lesser fuel quantity injected. The lower cooling effect of alcohols at low engine loads resulted in minor variations in the in-cylinder pressure compared to higher engine loads.

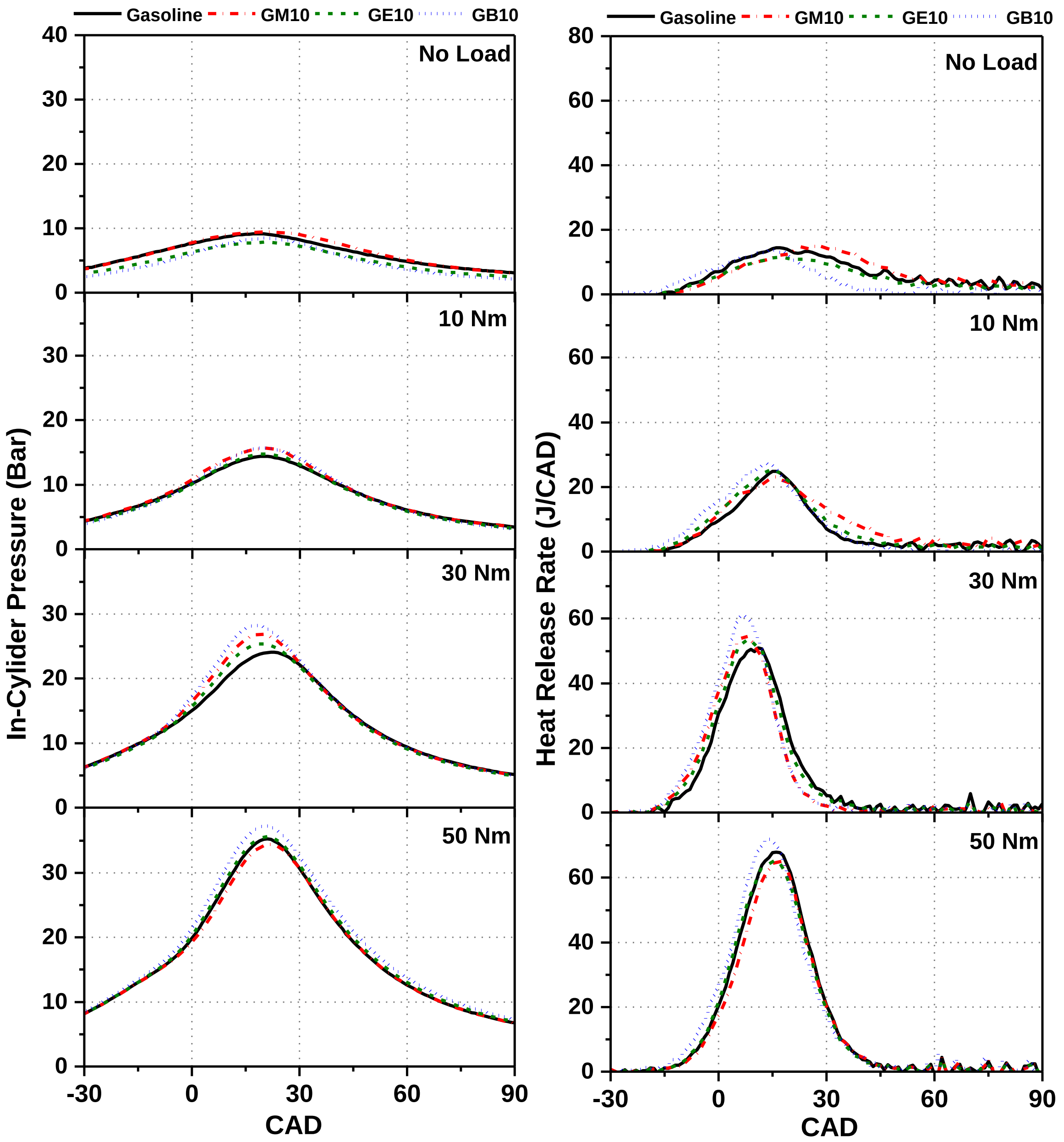

(a) (b)

Figure 3: (a) In-cylinder pressure rise and (b) heat release rate variations w.r.t. crank angle at different engine loads at 2500 rpm

GM10 had slightly higher P_{max} than other gasohols due to higher fuel-air mixture reactivity and oxygen content in methanol. Gasohols exhibited superior combustion at a medium engine load (30 Nm) than gasoline. GB10 exhibited the highest Pmax among different test fuels, followed by GM10 and then GE10. Gasohols exhibited superior combustion characteristics in the mid-load range due to relatively wider flammability limits and higher flame velocity than gasoline [36]. A relatively higher hydrophilic tendency of ethanol might be another reason for the lowest in-cylinder pressure for GE10, where moisture absorbed a fraction of combustion generated heat. At higher engine loads (50 Nm), GB10 exhibited the highest P_{max} due to higher calorific value and lower latent heat of vaporisation of butanol among all primary alcohols. However, other test fuels (GM10 and GE10) exhibited almost similar P_{max} as gasoline. A richer gasohol-air mixture at higher engine loads improved the combustion, leading to higher P_{max} than baseline gasoline [37]. Figure 3(b) exhibits HRR variations in the engine fueled with gasohols vis-à-vis baseline gasoline at various loads. HRR was calculated by applying the first law of thermodynamics to the in-cylinder pressure data [38]. For all test fuels, increasing engine load (up to 30 Nm) resulted in advanced maximum HRR (HRR_{max}) due to rapid charge combustion kinetics, which resulted in a shorter ignition delay. However, at 50 Nm engine load, the dominant charge-cooling effect led to slightly retarded HRR_{max} than at 30 Nm. HRR trends exhibited relatively higher HRR_{max} of GM10, GE10, and GB10 than gasoline at most engine loads. This was due to inherent fuel oxygen in alcohols, which promoted rapid heat release during combustion. Tian et al. [39] also reported a similar trend. This effect was not noticeable at no load; however, it was significant at higher loads due to the increased fuel quantity burned. At no load, all test fuels exhibited similar HRR trends with comparable HRR_{max}. At no load, the HRR_{max} of GM10 shifted towards after top dead centre (aTDC) side, which reflected slower charge combustion kinetics. However, GB10 exhibited the most advanced SoC with a shorter CD. At a higher engine load, the height of the HRR curve increased, and its width decreased. Increasing the height of the HRR curve exhibited relatively faster charge combustion kinetics, which supported the findings of in-cylinder pressure analysis as well. Reduced width of the HRR curve with increasing engine load exhibited somewhat shorter CD at higher engine loads. At mid-load (30 Nm), GB10 exhibited the maximum HRR_{max} amongst all test fuels. Relatively lower latent heat of vaporisation of butanol and higher reactivity were the main reasons for these trends, which became more dominant at higher loads. At medium loads, GM10 and GE10 showed somewhat higher HRR than gasoline. However, at higher loads (50 Nm), GM10 and GE10 showed relatively lower HRR_{max} than baseline gasoline. A dominant effect of higher latent heat of vaporisation of methanol and moisture availability in ethanol may be probable reasons for this trend.

Figure 4 shows SoC, CP, and CD variations of gasohols and gasoline-fueled engines at varying loads at 2500 rpm. Variations in SoC, CP, and CD of gasohols and gasoline-fueled engines at various speeds at fixed engine load are given in the Supporting information (Figure S2). These parameters were calculated from the mass fraction burned (MFB) analyses. SoC was calculated from the cumulative heat release (CHR) curve as the crank angle corresponding to 10% CHR. The crank angle corresponding to 90% CHR was defined as the end of combustion (EoC). The crank angle degree difference between the EoC and SoC was defined as the CD. Figure 4 shows that SoC advanced slightly with increasing engine load (up to 30 Nm) and then retarded slightly with further increasing engine load. At higher in-cylinder temperature conditions, relatively rapid charge combustion kinetics resulted in advanced SoC up to medium loads. However, the charge cooling effect became dominant at higher loads, leading to slightly retarded SoC. Relatively advanced SoC of gasohols than baseline gasoline was another important observation. This showed relatively superior combustion of gasohols due to its higher research octane number (RON) and inherent fuel oxygen content than gasoline. Among different gasohols, GM10 and GE10 exhibited retarded SoC than GB10. Relatively higher latent heat of vaporisation of methanol led to more significant charge cooling. The moisture in the ethanol resulted in somewhat slower fuel-air combustion kinetics than GB10.

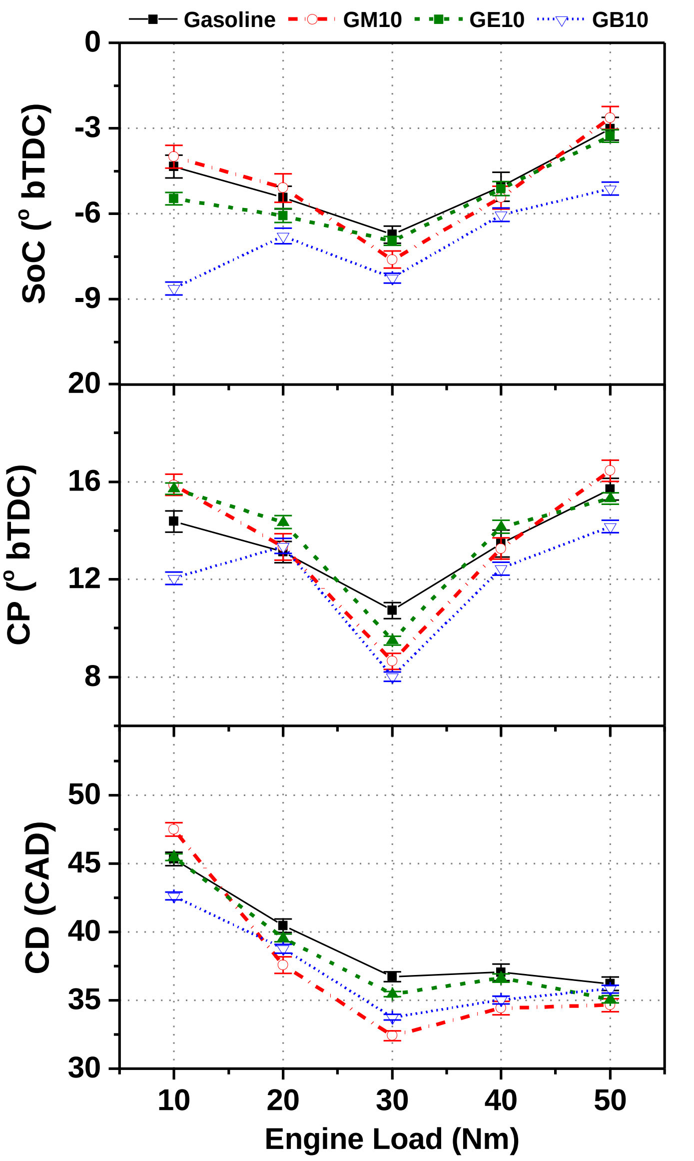

Figure 4: SoC, CP, and CD at varying engine loads at 2500 rpm

CP was another combustion parameter that affected the combustion stability since too advanced or retarded CP led to inferior engine performance and emissions. CP was calculated using MFB analysis, where the crank angle position corresponding to 50% CHR was considered CP. CP followed a trend similar to SoC for all test fuels, which advanced with increasing engine load up to 30 Nm and then retarded with further increasing engine load. Like SoC, the relative dominance of charge combustion kinetics and fuel properties were important for this trend. CP of gasohols (except GB10) exhibited a close relationship with load variations, slightly retarded at lower loads; however, CP of gasohols exhibited relatively advanced CP at higher loads. The difference among CP of various test fuels was the maximum at 30 Nm due to a trade-off between charge combustion kinetics and test fuel properties. Results showed that GM10 and GE10 exhibited relatively retarded CP than GB10 and baseline gasoline. Relatively higher latent heat of vaporisation of methanol and ethanol than butanol might be a vital reason for this behaviour, which led to relatively slower charge combustion kinetics. GB10 exhibited relatively advanced CP at all engine loads than other test fuels. This was mainly due to the relatively higher reactivity of butanol (higher cetane number of butanol than methanol and ethanol). This trend was reported by other researchers also [32]. CD was another important parameter that affected the engine performance and emissions. With increasing engine load (up to 30 Nm), CD reduced and remained constant until the maximum engine load. Relatively faster charge combustion kinetics in the presence of higher in-cylinder temperature might be a probable reason for shorter CD at higher loads. However, at 40 and 50 Nm, more fuel in the combustion chamber takes longer to burn completely, leading to a relatively longer CD than lower engine loads. Due to the integrated impact of these two counter-effects, charge combustion kinetics and the presence of higher fuel quantity, CD remained almost constant (for gasoline and GE10) or slightly increased (for GM10 and GB10) at higher loads. More heat losses from the cylinder walls at higher loads because of higher in-cylinder temperatures may be another parameter accountable for a relatively higher CD. Gasohols showed relatively lower CD than baseline gasoline. This was mainly because of the integrated impact of higher flame speed of alcohols, faster charge combustion kinetics, and fuel-bound oxygen, which resulted in rapid heat release from gasohols. Relatively lower CD of gasohol results in lower soot formation, which is discussed in the second part of this study. GM10 showed a relatively shorter CD than other gasohols and gasoline among different gasohols. The faster flame speed of methanol than ethanol and butanol may be responsible for this trend [40] [41]. However, at a lower load (10 Nm), the dominant influence of higher latent heat of vaporisation of methanol led to a slightly longer CD of GM10 than other test fuels.

3.2 Performance Characteristics

Figure 5 shows the performance characteristics (BTE, BSEC, and EGT) of the engine fueled with gasohols and baseline gasoline at varying engine loads. The effect of speed on the performance characteristics is given in the supporting information (Figure S3). Results showed that BTE improved with increasing engine load for all test fuels. A possible reason may be higher in-cylinder temperature, which increased with increasing injected fuel quantity. At higher loads, increased fuel quantity led to greater charge cooling, resulting in slightly higher volumetric efficiency, which may be one more probable reason for the higher BTE. This study exhibited that gasohols offer higher BTE than baseline gasoline [42]. This trend resulted in superior fuel characteristics of alcohols, such as higher latent heat of vaporisation and fuel-bound oxygen. The latent heat of vaporisation directly affected the charge cooling in the intake manifold. Higher latent heat of vaporisation resulted in increased intake charge density, leading to higher volumetric efficiency. Improved volumetric efficiency also led to complete combustion and higher BTE.

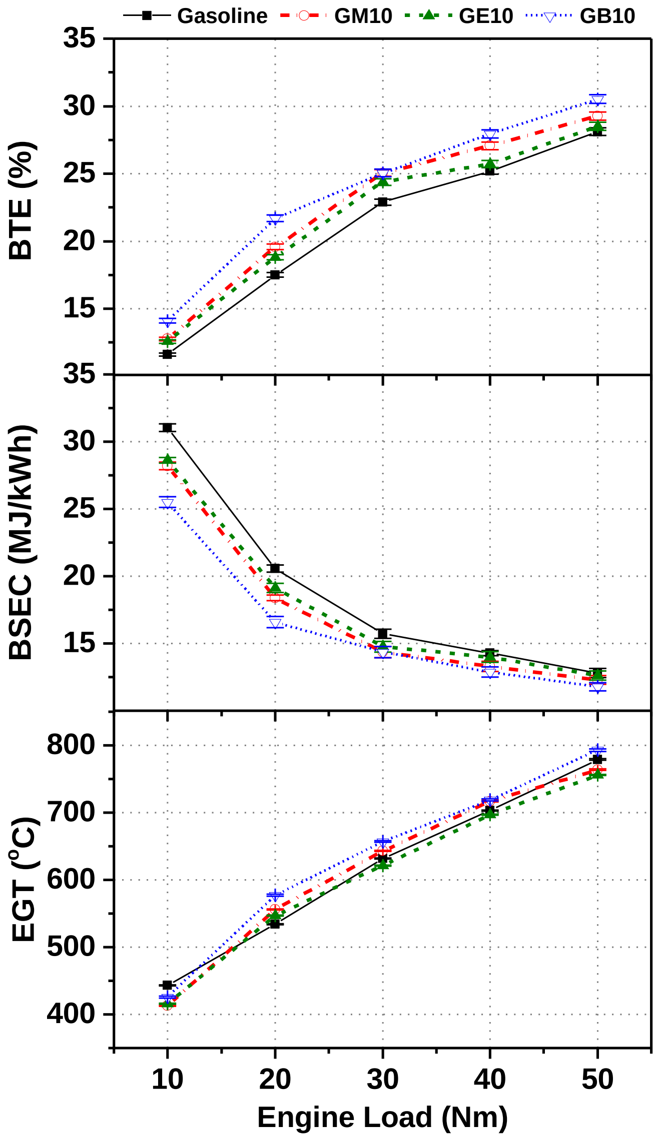

Figure 5: BTE, BSEC, and EGT at varying engine loads at 2500 rpm

GB10 showed the highest BTE, and GE10 showed the lowest BTE among gasohols due to relatively lower latent heat of vaporisation of butanol, higher charge reactivity, and availability of fuel-bound oxygen. BTE of GM10 was lower due to relatively higher latent heat of vaporisation of methanol; however, the moisture content of ethanol may be accountable for the slightly lower BTE of GE10. BSEC trends were the reverse of BTE trends for all test fuels. Gasohols exhibited relatively lower BSEC than gasoline. Among various gasohols, GB10 showed the lowest BSEC. EGT is measured as a qualitative parameter, which indicates the in-cylinder temperature. Higher in-cylinder temperature restricts the condensation of volatile species. This resulted in a relatively lesser contribution of larger particles, leading to lower total particulate matter (TPM) emissions. Higher EGT represents superior combustion, causing higher NOx and lower soot formation. Other effects of EGT on particulate emissions have been discussed in detail in the second part of this study. EGT trends were similar for all test fuels, and they increased with increasing load. More fuel quantity burnt in the combustion chamber at higher loads led to higher peak in-cylinder temperature, causing a higher EGT. At 10 Nm torque, the EGT of gasohols was slightly lower than baseline gasoline. The combined effect of lower in-cylinder temperature and charge cooling due to gasohols might be reasons for this trend. At higher engine loads, GB10 exhibited the highest EGT due to superior combustion, which could also be seen in BTE trends. GM10 showed relatively higher EGT than GE10 and baseline gasoline at medium loads. Relatively higher oxygen content and faster flame velocity might be probable reasons for this trend, which improved the combustion more than GE10 and gasoline. At most test conditions, the impact of moisture traces in ethanol was noticeable in the EGT trend of GE10, which absorbed a significant fraction of combustion heat release, resulting in lower EGT than other gasohols.

3.3 Regulated Emissions Characteristics

Figure 6 shows CO, HC, and NOx emitted by gasohols fueled and gasoline engines at varying loads. The effect of engine speed on emission characteristics is given in supporting information (Figure S4). For emissions characterisation, unprocessed emission concentrations of CO, HC, and NOx were obtained in ppm. Using established equations, these emission concentrations were converted to mass emissions (g/kWh) [43].

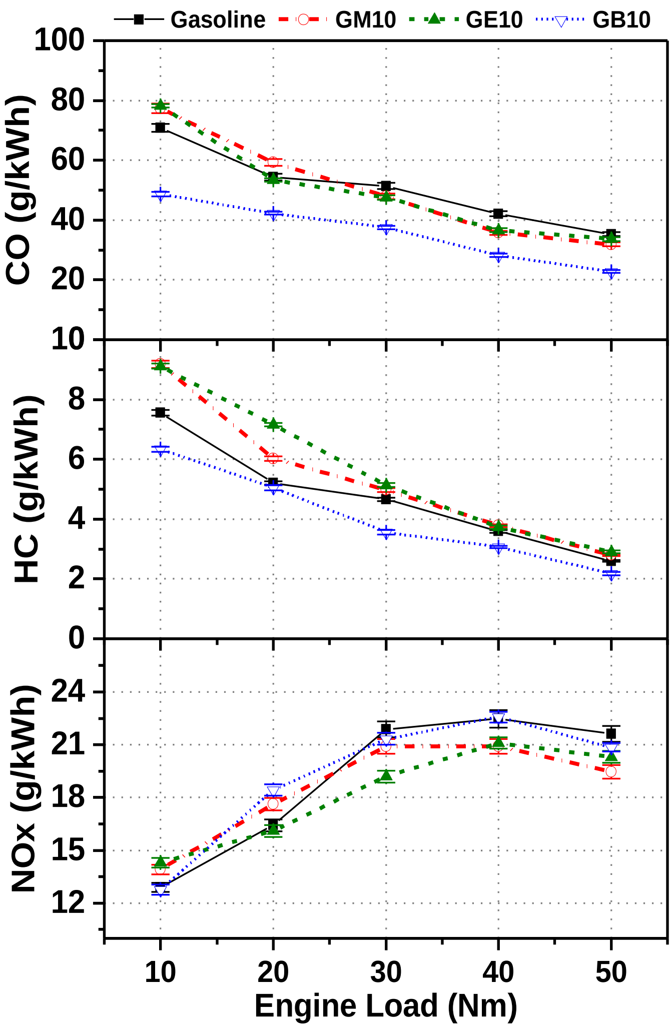

Figure 6: Mass emissions of CO, HC, and NOx at varying engine loads at 2500 rpm

CO emission was reduced with increasing engine load for all test fuels. More CO-to-CO_2 oxidation due to comparatively higher in-cylinder temperature was a major cause for lower CO emission at higher engine loads. At higher loads, gasohols emitted lower CO. Higher loads improved CO-to-CO_2 oxidation due to the combined effect of higher in-cylinder temperatures and inherent fuel oxygen, which reduced CO emission from gasohols [44]. However, at lower loads, the dominant charge cooling effect of GM10 and GE10 caused relatively lower in-cylinder temperatures, leading to higher CO emissions. A relatively higher H/C ratio of gasohols compared to baseline gasoline might be another reason for lower CO emission because test fuel with a higher H/C ratio emits lower CO. Amongst different gasohols, GB10 fueled engines emitted significantly lower CO emission. This may be because of the lower latent heat of vaporisation and higher chemical reactivity of butanol, among other alcohols, which resulted in superior combustion of GB10.

At lower loads, the dominant charge cooling effect of GM10 and GE10 further reduced the in-cylinder temperatures, hence increasing the CO emission. However, this effect was not as dominant as the engine load due to the higher in-cylinder temperature and increased injected fuel quantity for meeting the load requirement. For all test fuels, HC emissions were also reduced with increasing load. Among various HC sources, incomplete combustion of fuel and fuel trapped in crevices were the main source in the SI engines. Higher in-cylinder temperature resulted in superior combustion, reducing HC emissions at higher loads. Results showed that GM10 and GE10 produced higher HC emissions than baseline gasoline, especially at lower loads. However, HC emissions from the engine fueled with GB10 were relatively lower than baseline gasoline. This may be due to the lower heat of vaporisation and higher heating value of butanol than methanol and ethanol. Relatively lower in-cylinder temperature because of the cooling effect of GM10 and GE10 was the main reason for incomplete combustion, resulting in higher HC emissions. HC emissions from GM10, GE10, and gasoline-fueled engines were almost similar at higher loads. GB10 showed the lowest HC emissions due to advanced CP compared to other test fuels. Figure 6 shows the NOx emissions, which depend on three factors: oxygen availability, peak combustion temperature, and the time available at high-temperature conditions. Increasing load led to relatively higher NOx emissions. This was because of relatively higher in-cylinder temperature at higher loads, which provided more favourable conditions for NOx emission formation. However, higher in-cylinder temperature improved the soot oxidation. It showed no increment in soot emission at higher engine loads, presented in detail in the second part of this study. At the highest engine load (50 Nm), NOx emissions remained almost constant because of a trade-off between higher in-cylinder temperatures and lower oxygen presence (due to fuel-rich combustion). Relatively lower NOx emissions from gasohols than baseline gasoline was a major finding of this study. This was more prominent at higher loads due to the dominant charge cooling nature of alcohol, which reduced the peak in-cylinder temperature [45]. As the laminar flame speed of alcohols is higher, blending alcohols to gasoline shortens the CD, reducing the NOx formation. GB10 exhibited relatively higher NOx emissions among different gasohols than GM10 and GE10. Relatively lower latent heat of vaporisation and higher reactivity of butanol were possible factors for relatively lower NOx emissions from GB10. This can also be observed in engine performance trends, where GB10 exhibited higher BTE and EGT (Figure 5).

3.4 Unregulated Emission Characteristics

Unregulated emission species are the intermediate incomplete combustion products of saturated HCs and oxygenated compounds of the test fuels. These unregulated species are extremely harmful to human health upon prolonged exposure [11]. Hence it is important to investigate the emission of unregulated species from the engine using alternative fuels such as primary alcohols on a large scale. An FTIR emission analyser was used to measure unregulated emission species in this study. The FTIR emission analyser can measure 31 unregulated emission species, out of which 14 species are reported in this paper. The remaining 17 species are not discussed because those species were below the detection limit of the analyser.

3.4.1 Emissions of various Oxides of Nitrogen, Sulphur, and Ammonia

The first group of unregulated emission species included different oxides of nitrogen, namely nitric oxide (NO), nitrogen dioxide (NO_2), nitrous oxide (N_2O) emitted by gasohols, and gasoline-fueled engines (Figure 7). NO, NO_2, and N_2O are cumulatively known as NOx, a regulated emission. However, they are unregulated emissions when each species is measured separately. NO, contribute to a large fraction of NOx. NO_2 is a more toxic gaseous species than NO, and its exposure leads to respiratory diseases. N_2O, also known as "laughing gas," is a strong greenhouse gas that destroys the ozone layer and affects the human body adversely. Figure 7(a) shows NO, NO_2, and N_2O emissions from gasohols and gasoline-fueled engines at varying engine loads at 2500 rpm. The effect of engine speed on NO, NO_2, and N_2O emissions is given in supporting information (Figure S5). It was found that a significant amount of NO was emitted from all test fuels. NO emission increased with increasing engine load due to increasing peak in-cylinder temperature. Each test fuel exhibited similar NO emissions trends at lower loads, while the gasohols-fueled engine produced lower NO emissions at higher loads. This was because of the dominant effect of peak in-cylinder temperature on NO formation [38]. Similar findings were reported by Agarwal et al. [30].

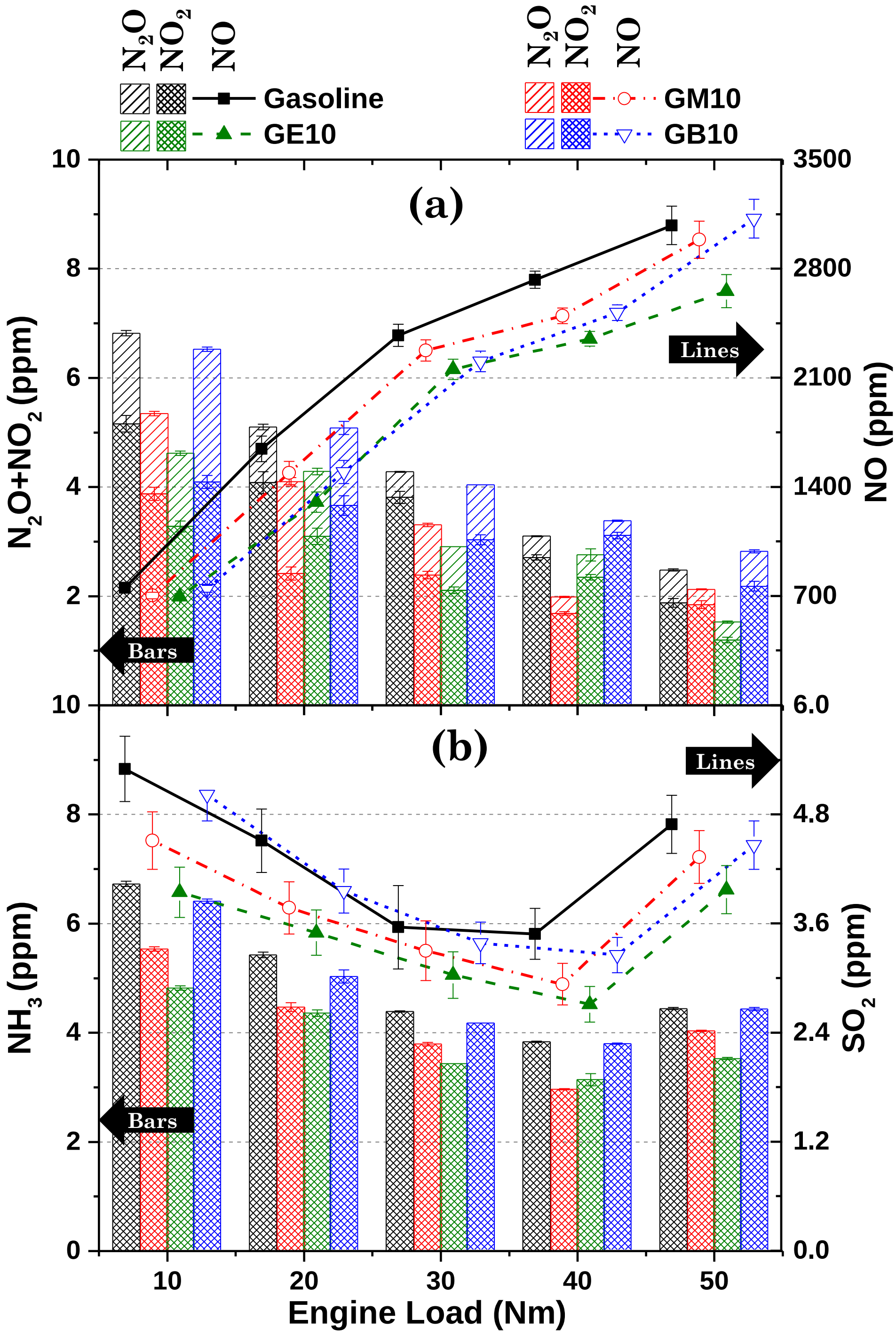

Figure 7: (a) Various oxides of nitrogen, (b) sulfur dioxide, and ammonia traces emitted at varying engine loads at 2500 rpm

Among different gasohols, the GE10-fuelled engine produced significantly reduced NO than GM10 and GB10. The availability of moisture in the ethanol may be a possible reason for this trend, which absorbed a significant fraction of combustion energy, leading to lower peak in-cylinder temperature. GM10 and GB10 have almost identical NO emissions but are relatively lower than gasoline. NO_2 and N_2O emissions were relatively insignificant, and they were reduced with increasing engine load for all test fuels. NO_2 is formed during combustion via several chemical mechanisms, in which oxidation of existing NO might be an important one [46]. NO_2 was formed mainly at lower in-cylinder temperatures, and reverse conversion of NO_2 to NO took place at a temperature >1200 K in the engine combustion chamber [47]. This reduced the NO_2 emission and increased the NO emission with increasing engine load. Gasohols showed relatively lower NO_2 emissions than gasoline due to lower NO formation. Gasohols exhibited higher N_2O emissions than baseline gasoline; however, the difference was statistically insignificant. The higher cooling effect of gasohols provided favourable conditions for N_2O formation.

Figure 7(b) shows a comparison of Sulphur dioxide (SO_2) and ammonia (NH_3) emissions for gasohols and gasoline-fueled engines at varying engine loads. The effect of engine speed on SO_2 and NH_3 emissions is given in supporting information (Figure S5). SO_2 is formed in the engine cylinder during combustion because of reactions between fuel Sulphur and atmospheric oxygen. Sometimes lubricating oil leaks into the combustion chamber and thio-compounds in lubricating oil contributes to SO_2 emission. NH_3 is a toxic gas that affects human health adversely. It also acts as a secondary particulate matter precursor. A higher concentration of these species deteriorates the urban air quality and is hazardous to human health; however, concentrations of these species reported in this study were negligible. For all test fuels, SO_2 emissions decreased with increasing engine load. A previous study reported a similar observation that SO_2 emission was reduced for richer fuel-air mixtures and vice-versa [48].

At 50 Nm engine load, a higher burning/ pyrolysis of lubricating oil in the engine combustion chamber resulted in higher SO_2 emission. Fuels such as gasoline having higher Sulphur content emit more SO_2 in the engine exhaust. Results show that gasohols emitted relatively lower SO_2 emissions due to reduced Sulphur content because of alcohol blending to gasoline. GE10 shows the lowest SO_2 emission among different gasohols. NH_3 emission showed a similar trend to SO_2 emission for all test fuels. NH_3 emission was significant at lower loads, which reduced with increasing load (Figure 7b). Gasohols showed relatively lower NH_3 emissions. GE10 exhibited the lowest NH_3 emission at all gasohols at all loads, although the difference was insignificant.

3.4.2 Emissions of Formaldehyde, Formic acid, and Isocyanic acid

The second group of unregulated species included Formaldehyde (HCHO), Formic acid (HCOOH), and Isocyanic acid (HNCO) emitted by gasoline and gasohol-fueled engine at varying loads (Figure 8). The effect of engine speed on HCHO, HCOOH, and HNCO emissions is given in supporting information (Figure S6). HCHO, an intermediate combustion product, is a carcinogenic air pollutant. HCHO formation depends on several factors, such as in-cylinder temperature and residence time of HCs in the exhaust [49]. HCOOH is another harmful unregulated emission species, damaging the central nervous system leading to coma and death [32]. The presence of oxygen in the engine exhaust in lean conditions and EGT has a major impact on the formation of HCOOH. HCOOH formation is independent of EGT under fuel-rich conditions [32]. Literature shows that EGT has an inverse relationship with HCOOH formation under lean and stoichiometric in-cylinder conditions [33], indicating that oxygen in the engine exhaust affects the HCOOH formation. When EGT is low, HCOOH emissions are generally high. The presence of higher temperatures promotes the decomposition of HCOOH into other by-products. It was also observed that oxygenated fuel enhances HCOOH formation because they allow HCOOH precursors to originate from HCs [32]. HNCO is formed by photochemical ageing of exhaust under idle and high load conditions.

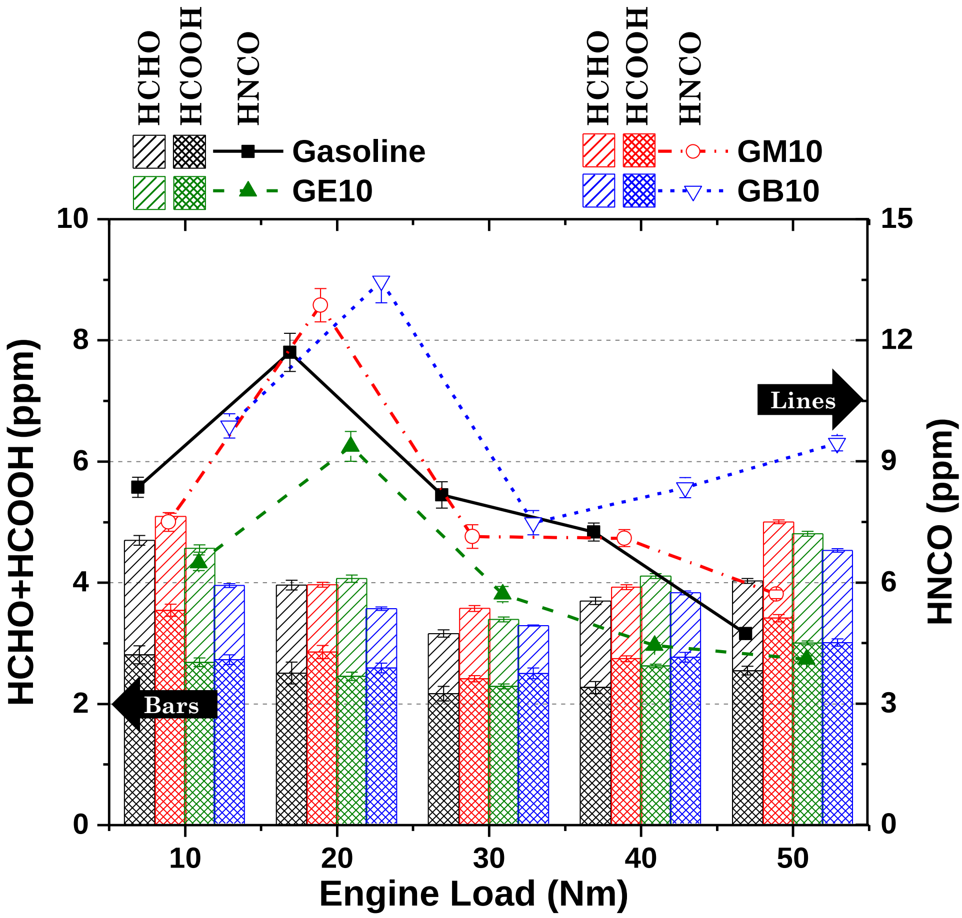

Figure 8: Formaldehyde, formic acid, and isocyanic acid emitted at different engine loads at 2500 rpm

It was observed that as engine load increased, HCHO emission reduced up to a certain extent and then increased with a further increase in load [50]. This showed that in-cylinder temperature has a dominant effect on HCHO formation at lower engine loads. HCHO emission reduces due to complete combustion at medium engine loads. However, lack of oxygen under high engine load conditions hinders combustion, leading to higher HCHO emissions. The cooling effect of gasohols was also visible in the HCHO trends, which exhibited that the gasohol-fueled engine produced somewhat higher HCHO than the baseline gasoline-fueled engine [51]. Among different gasohols, the GM10-fueled engine emitted the highest traces of HCHO because of the higher latent heat of vaporisation of methanol, among other alcohols. Trends of HCOOH emission were similar to HCHO emission because HCOOH was mainly produced by OH radicals [36]. Similar to

HCHO emission, the GB10-fuelled engine emitted the lowest HCOOH. The reason behind such a trend was higher EGT, which promoted the decomposition of HCOOH into other by-products. GE10 emitted comparatively higher HCOOH because of moisture traces in ethanol. HNCO emission increased slightly with increasing engine load and then decreased with a further increase in the engine load. HNCO was mainly formed due to reaction with CO and NO in high-temperature conditions and noble metal-based catalysts used in the emission after-treatment/control devices. At most loads, the gasohol-fueled engine produced lower HNCO than baseline gasoline. HNCO emission was dominantly affected by the EGT, which was also seen in HNCO trends of different gasohols. Among other test fuels, GE10 emitted the lowest HNCO emission due to relatively lower EGT, which promoted the formation of HNCO.

3.4.3 Emissions of Unsaturated and Aromatic HCs

Figure 9(a) shows the concentrations of unsaturated HCs produced from gasohol- and gasoline-fueled engines at varying loads. The effect of engine speed on Acetylene (C_2H_2), Ethylene (C_2H_4), and Propene (C_3H_6) emissions is given in supporting information (Figure S7). Incomplete fuel combustion is the main source of emissions of unsaturated HCs such as C_2H_2, C_2H_4, C_3H_6, etc. It is desirable to have low C_2H_2 emissions because it acts as a soot precursor. C_2H_2 originates from C_2H_4, a volatile organic carbon (VOC) [11]. C_2H_4 leads to the formation of smog after reacting with NOx. For all test fuels, C_2H_2 emission decreased with increasing engine load. This may be because of higher in-cylinder temperature, which promoted the oxidation of these intermediate combustion products, leading to lower C_2H_2. The gasohol-fueled engine produced somewhat lower traces of C_2H_2 than baseline gasoline. The possible reason could be a smaller carbon chain in gasohols [7]. Lower C_2H_2 results in lower soot formation for gasohol fuelled engines because C_2H_2 acts as a precursor during soot formation. Similar to C_2H_2, C_2H_4 and C_3H_6 emissions were also reduced with increasing engine load. The gasoline-fueled engine emitted a relatively higher C_2H_4 and C_3H_6 than gasohols, leading to higher soot emissions. Complete combustion due to inherent fuel oxygen and faster fame velocity might be possible reasons for lower emissions of unsaturated HCs [11]. The trend of C_2H_4 emission from GM10 also validated the reason mentioned above, which exhibited the lowest C_2H_4 emission.

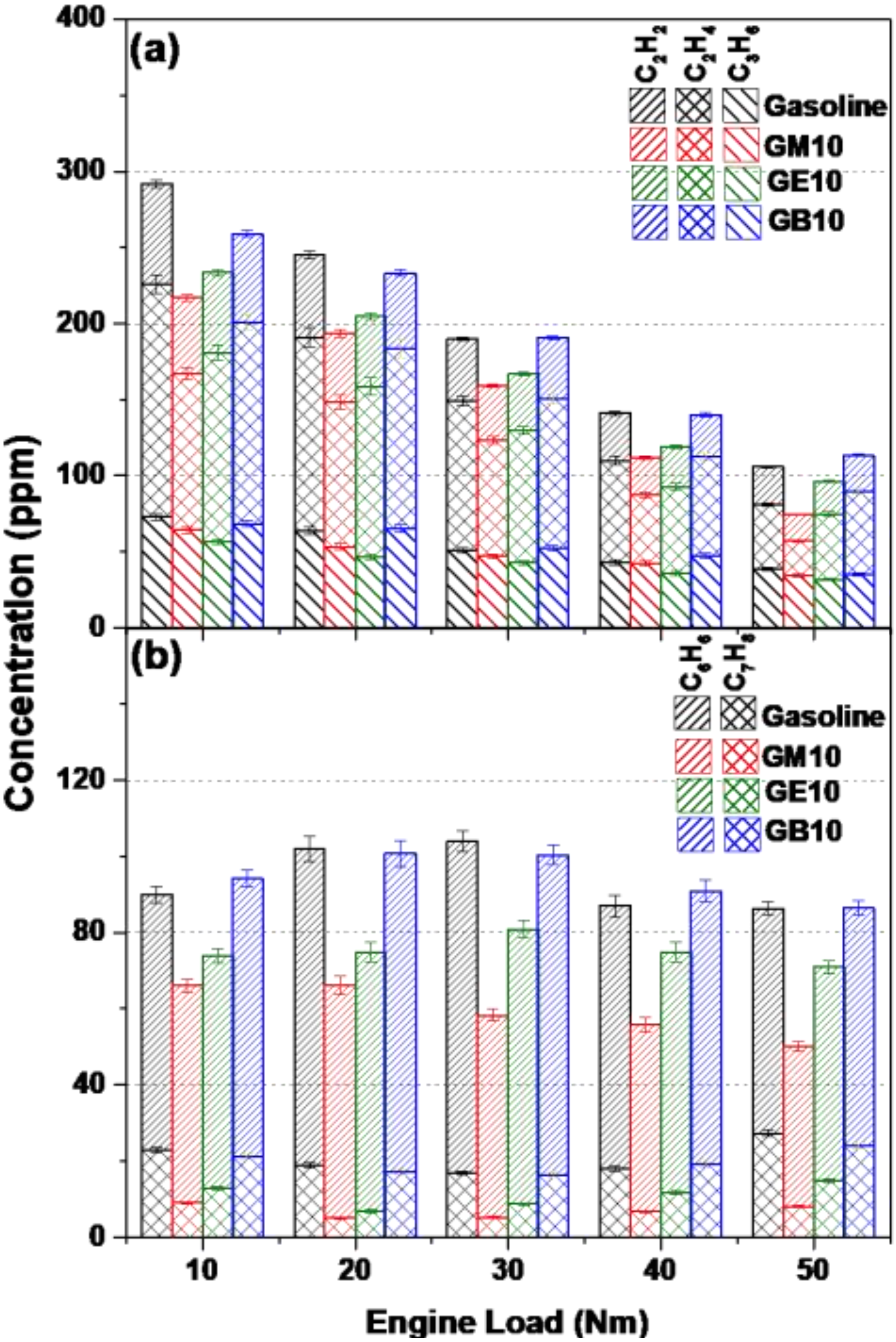

Figure 9: (a) Unsaturated and (b) aromatic HCs emitted at varying engine loads at 2500 rpm

Figure 9b shows the Benzene (C_6H_6) and Toluene (C_7H_8) emissions from gasohols and gasoline-fueled engines at various loads at a constant speed of 2500 rpm. The effect of engine speed on C_6H_6 and C_7H_8 emissions is given in supporting information (Figure S7). Benzene and Toluene are reactive organic compounds, mainly originating from unburnt fuel and pyro-synthesis processes during combustion [52]. Benzene is formed due to unburnt fuel and reactions between the aromatic and non-aromatic compounds formed during combustion. An increasing load produced comparatively lower benzene emission; however, benzene emission concentration increased slightly at the highest engine load. Gasohol-fueled engines emitted relatively lower benzene traces compared to baseline gasoline. This was mainly due to gasoline substitution by alcohol, which does not contain benzene [7]. Gasohols accelerated the conversion of CO to CO_2 because of fuel oxygen and reduced benzene emissions [53]. GM10 showed the lowest benzene emissions among different test fuels due to the highest fuel oxygen content in methanol, which hampered benzene ring formation in oxygen (O_2) deficient zones of the combustion chamber. Unsaturated HCs constituents of fuel are also accountable for producing C_6H_6 and C_7H_8. Methanol does not contain these compounds, and the same results can be seen in benzene and toluene emission trends [51]. Engine emitted higher C_7H_8 emissions with increasing load up to medium loads, which reduced with further increasing load [51]. C_7H_8 emissions increased slightly because of the higher fuel quantity injected with increasing engine load [53]. GM10 exhibited the lowest C_7H_8 emissions for all engine loads among different gasohols due to methanol's highest fuel oxygen content.

Conclusions

In this study, experiments were carried out to compare the combustion, performance, and emission characteristics of a SI engine fueled with different gasoline-alcohol blends (GM10, GE10, and GB10) vis-à-vis baseline gasoline. Combustion results exhibited that the gasohol-fueled engine had relatively higher in-cylinder pressure than baseline gasoline. GB10 showed the highest BTE amongst all test fuels, dominant at higher loads. BSEC was the lowest for GB10 and the highest for gasoline. Regulated emissions of CO, HC, and NOx were lower from gasohols compared to gasoline. HCHO emission of the gasohol-fueled engine was relatively lower than gasoline due to improved combustion and oxidation. HCOOH and HNCO emissions were insignificant for all test fuels. NO emission trends of gasohol and baseline gasoline exhibited a significant difference because of relatively higher latent heat of vaporisation of gasohols, which lowered the peak in-cylinder temperature, leading to lower NO emission than gasoline. NO_2 and N_2O emissions are insignificant for all test fuels. NH_3 and SO_2 emissions emitted by the gasohol-fueled engine were also relatively lower than gasoline. Gasohols showed lower unsaturated HC and aromatic HC emissions. Alcohols have a bright future for their use in SI engines, and they can partially replace gasoline. The GB10-fuelled engine showed significant improvement in engine performance and combustion characteristics, and it can reduce regulated emissions than other test fuels. Overall, this study demonstrated that butanol has significant potential to displace gasoline partially.

Availability of Data

The experimental data that support the findings/results of the present study are available with the corresponding author upon reasonable request.

Supporting Information

S1. Combustion Characteristics at Different Engine Speeds

S2. Performance Characteristics at Different Engine Speeds

S3. Emission Characteristics at Different Engine Speeds

S4. Unregulated Emission Characteristics at different Engine Speeds

- S4.1 emission of oxides of nitrogen, sulfur dioxide, and ammonia
- S4.2 Emissions of formaldehyde, formic acid, and isocyanic acid
- S4.3 emission of unsaturated and aromatic hydrocarbons

Author Information

Corresponding Author

Avinash Kumar Agarwal, Indian Institute of Technology Kanpur, Kanpur-208016, India, ORCID: https://orcid.org/0000-0002-7777-785X;

Email: akag@iitk.ac.in

Authors

Akhilendra Pratap Singh, Indian Institute of Technology Kanpur, Kanpur-208016, India, ORCID: https://orcid.org/0000-0001-5742-1517

Utkarsha Sonawane, Indian Institute of Technology Kanpur, Kanpur-208016, India, ORCID: https://orcid.org/0000-0002-3592-3417

References

1. José, G., Johansson, T.B., Reddy, A.K.N., Williams, R.H. Energy for the new millennium. Ambio: A journal of the human environment 2011; 30(6): 330-338.
2. Pardiwala, J.M., Patel, F., Patel, S. Review paper on catalytic converter for automotive exhaust emission. Gas 2011; 18: 19.
3. Mukherjee, A., Roy, K., Bagchi, J., Mondal, K. Catalytic Converter in Automobile Exhaust Emission. Journal for Research 2016; 2(10).
4. Sequera AJ, Parthasarathy RN, Gollahalli SR. Effects of fuel injection timing in the combustion of biofuels in a diesel engine at partial loads. Journal of energy resources technology. 2011 Jun 1;133(2).
5. Issayev, G., Sarathy, S.M., Farooq, A. Auto-ignition of diethyl ether and a diethyl ether/ethanol blend. Fuel 2020; 279:118553.
6. Maurya, RK and Agarwal, A.K., 2015. Experimental investigations of particulate size and number distribution in an ethanol and methanol-fueled HCCI engine. Journal of Energy Resources Technology, 137(1).

7. Pellegrini, L.A., Soave, G., Gamba, S., Langè, S. Economic analysis of a combined energy–methanol production plant. Applied energy 2011; 88(12): 4891-4897.
8. Li, H., Hong, H., Jin, H., Cai, R. Analysis of a feasible polygeneration system for power and methanol production taking natural gas and biomass as materials. Applied Energy 2010; 87(9): 2846-2853.
9. Li, Y., Bai, X., Tuner, M., Im, H.G., Johansson, B. Investigation on a high-stratified direct injection spark ignition (DISI) engine fueled with methanol under a high compression ratio. Applied Thermal Engineering 2019; 148:352-362.
10. Zhen X, Wang Y. An overview of methanol as an internal combustion engine fuel. Renewable and Sustainable Energy Reviews. 2015 Dec 1; 52:477-93.
11. Bielaczyc, P., Woodburn, J., Klimkiewicz, D., Pajdowski, P., Szczotka, A. An examination of the effect of ethanol-gasoline blends' physicochemical properties on emissions from a light-duty spark-ignition engine. Fuel Processing Technology 2013; 107: 50-63.
12. Wei, Y., Wang, K., Wang, W., Liu, S. and Yang, Y., 2014. Contribution Ratio Study of Fuel Alcohol and Gasoline on the Alcohol and Hydrocarbon Emissions of a Gasohol Engine. Journal of Energy Resources Technology, 136(2).
13. Bata, R.M., Elrod, A.C., Lewandowskia, T.P. Butanol as a blending agent with gasoline for IC engines. SAE Technical Paper 1989; 890434.
14. Gautam, M. and Martin, D.W., 2000. Combustion characteristics of higher-alcohol/gasoline blends. Proceedings of the Institution of Mechanical Engineers, Part A: Journal of Power and Energy, 214(5), pp.497-511.
15. Zhen X, Wang Y, Liu D. Bio-butanol as a new generation of clean alternative fuel for SI (spark ignition) and CI (compression ignition) engines. Renewable Energy. 2020 Mar 1; 147:2494-521.

16. Sharma N, Agarwal RA, Agarwal AK. Particulate bound trace metals and soot morphology of gasohol fueled gasoline direct injection engine. Journal of Energy Resources Technology. 2019 Feb 1;141(2).

17. Jiang Q, Zhang C, Jiang J. Reduction of NOx in a regenerative industrial furnace with the addition of methanol in the fuel. J. Energy Resour. Technol.. 2004 Jun 1;126(2):159-65.

18. Nord AJ, Hwang JT, Northrop WF. Emissions From a Diesel Engine Operating in a Dual-Fuel Mode Using Port-Fuel Injection of Heated Hydrous Ethanol. Journal of Energy Resources Technology. 2017 Mar 1;139(2).

19. Bata, R.M., Roan, V.P. Effects of ethanol and/ or methanol in alcohol-gasoline blends on exhaust emissions. Journal of Engineering for Gas Turbines and power 1989; 111(3): 432-438.

20. Sharma, N. and Agarwal, A.K., 2020. Effect of Fuel Injection Pressure and Engine Speed on Performance, Emissions, Combustion, and Particulate Investigations of Gasohols Fuelled Gasoline Direct Injection Engine. Journal of Energy Resources Technology, 142.

21. Brusstar, M.J., Gray, C.L. High efficiency with future alcohol fuels in a stoichiometric medium duty spark ignition engine. SAE Technical Paper 2007; 2007-01-3993.

22. Chen, Z., Wu, Z., Liu, J., Lee, C. Combustion and emissions characteristics of high n-butanol/diesel ratio blend in a heavy-duty diesel engine and EGR impact. Energy Conversion and Management 2014; 78: 787-795.

23. Abu-Zaid, M., Badran, O. and Yamin, J., 2004. Effect of methanol addition on the performance of spark-ignition engines. Energy & Fuels, 18(2), pp.312-315.

24. Canakci, M., Ozsezen, A.N., Alptekin, E., Eyidogan, M. Impact of alcohol–gasoline fuel blends on the exhaust emission of an SI engine. Renewable Energy 2013; 52: 111-117.

25. Eyidogan, M., Ozsezen, A.N., Canakci, M., Turkcan, A. Impact of alcohol–gasoline fuel blends on the performance and combustion characteristics of an SI engine. Fuel 2010; 89(10): 2713-2720.

26. Prasad, B.S.N., Pandey J.K., Kumar, G.N. Impact of changing compression ratio on engine characteristics of an SI engine fueled with equi-volume blend of methanol and gasoline. Energy 2020; 191: 116605.

27. Yücesu, H.S., Topgül, T., Cinar, C., Okur, M. Effect of ethanol-gasoline blends on engine performance and exhaust emissions in different compression ratios. Applied Thermal Engineering 2006; 26(17-18): 2272-2278.

28. He, B., Wang, J., Hao, J., Yan, X., Xiao, J. A study on emission characteristics of an EFI engine with ethanol-blended gasoline fuels. Atmospheric Environment 2003; 37(7): 949-957.

29. Costagliola, M.A., Prati, M.V., Florio, S., Scorletti, P., Terna, D., Iodice, P., Buono, D., Senatore, A. Performances and emissions of a 4-stroke motorcycle fueled with ethanol/gasoline blends. Fuel 2016; 183:470-477.

30. Agarwal, A.K., Shukla, P.C., Gupta, J.G., Patel, C., Prasad, R.K., Sharma N. Unregulated emissions from a gasohol (E5, E15, M5, and M15) fueled spark-ignition engine. Applied energy 2015; 154: 732-741.

31. Li, Y., Ning, Z., Lee, C.F., Lee, T.H., Yan, J. Performance and Regulated/ Unregulated Emission Evaluation of a Spark-Ignition Engine Fueled with Acetone–Butanol–Ethanol and Gasoline Blends. Energies 2018; 11(5):1121.

32. Poulopoulos, S.G., Samaras, D.P., Philippopoulos, C. J. Regulated and unregulated emissions from an internal combustion engine operating on ethanol-containing fuels. Atmospheric environment 2001; 35(26): 4399-4406.

33. Liu, F.J., Liu, P., Zhu, Z., Wei, Y.J., Liu. S.H. Regulated and unregulated emissions from a spark-ignition engine fueled with low-blend ethanol-gasoline mixtures. Proceedings of the Institution of Mechanical Engineers, Part D: Journal of Automobile Engineering 2012; 226(4): 517-528.

34. Corral-Gómez L, Rubio-Gómez G, Rodriguez-Rosa D, Martín-Parra A, de la Rosa-Urbalejo D, Martínez-Martínez S. A comparative analysis of knock severity in a Cooperative Fuel Research engine using binary gasoline–alcohol blends. International Journal of Engine Research. 2020 May 11:1468087420916683.

35. Kalwar A, Singh AP, Agarwal AK. Utilisation of primary alcohols in dual-fuel injection mode in a gasoline direct injection engine. Fuel. 2020 Sep 15; 276:118068.

36. Aghahossein, S.S., Abdollahipoor, B., Windom, B., Reardon, K.F., Foust, T.D. Effects of blending C3-C4 alcohols on motor gasoline properties and performance of spark ignition engines: A review. Fuel Processing Technology 2020; 197: 106194.

37. Fan, Z., Xia, Z., Shijin, S., Jianhua, X. and Jianxin, W., 2010. Unregulated emissions and combustion characteristics of low-content methanol−gasoline blended fuels. Energy & fuels, 24(2), pp.1283-1292.

38. Heywood JB. Internal combustion engine fundamentals McGraw-Hill Book Company. New York. 1988.

39. Tian, Z., Zhen, X., Wang, Y., Liu, D., Li, X. Comparative study on combustion and emission characteristics of methanol, ethanol, and butanol fuel in TISI engine. Fuel 2020; 259: 116199.

40. Li, Q., Wu J., Huang, Z. Laminar flame characteristics of C1–C5 primary alcohol-isooctane blends at elevated temperature. Energies 2016; 9(7):511.

41. Prasad, B.S.N., Kumar G.N. Influence of ignition timing on performance and emission characteristics of an SI engine fueled with equi-volume blend of methanol and gasoline. Energy Sources, Part A: Recovery, Utilisation, and Environmental Effects 2019; 1-15.

42. Feng H, Xiao S, Nan Z, Wang D, Yang C. Thermodynamic Analysis of Using Ethanol—Methanol—Gasoline Blends in a Turbocharged, Spark-Ignition Engine. Journal of Energy Resources Technology. 2021 Dec 1;143(12).

43. Automotive Vehicles—Exhaust Emissions—Gaseous Pollutants From Vehicles Fitted With Compression Ignition Engines—Method of Measurement. IS-14273. 1999.

44. Zhang, C., Ge, Y., Tan, J., Peng, Z. and Wang, X., 2017. Emissions From Light-Duty Passenger Cars Fueled With Ternary Blend of Gasoline, Methanol, and Ethanol. Journal of Energy Resources Technology, 139(6)

45. Rice, R.W., Sanyal, A.K., Elrod, A.C. and Bata, R.M., 1991. Exhaust gas emissions of butanol, ethanol, and methanol-gasoline blends.

46. Wei, Y., Shenghua, L., Li H., Rui, Y., Jie, L., Ying W. Effects of methanol/gasoline blends on a spark-ignition engine performance and emissions. Energy & Fuels 2008; 22(2): 1254-1259.

47. Klimstra, J., Westing, J. NO_2 from lean-burn engines - On its lower sensitivity to leaning than NO. SAE Technical Paper 1995; 950158.

48. Rahim, A., Jaafar, NM, Nazri, M., Sapee, S., Elraheem, H.F. Effect on particulate and gas emissions by combusting biodiesel blend fuels made from different plant oil feedstocks in a liquid fuel burner. Energies 2016; 9(8): 659.

49. Zervas, E., Montagne, X., & Lahaye, J. C1−C5 Organic acid emissions from an SI engine: influence of fuel and air/fuel equivalence ratio. Environmental Science & Technology 2001; 35(13): 2746–2751.

50. Wei, Y., Liu, S., Liu, F., Liu, J., Zhu, Z. and Li, G., 2009. Formaldehyde and methanol emissions from a methanol/gasoline-fueled spark-ignition (SI) engine. Energy & fuels, 23(6), pp.3313-3318.

51. Yao, Dongwei, Xinchen Ling, and Feng Wu. Experimental investigation on the emissions of a port fuel injection spark ignition engine fueled with methanol–gasoline blends. Energy & Fuels 2016; 30(9): 7428-7434.

52. Wallner, T., Frazee, R. Study of regulated and non-regulated emissions from combustion of gasoline, alcohol fuels and their blends in a DI-SI engine. SAE Technical Paper 2010; 2010-01-1571.

53. Correa, S.M., Arbilla, G. Aromatic hydrocarbons emissions in diesel and biodiesel exhaust. Atmospheric Environment 2006; 40(35): 6821-6826.

Methanol/ Ethanol/ Butanol-Gasoline Blends Use in Transportation Engine: Combustion, Emissions, and Performance Study

Akhilendra Pratap Singh, Utkarsha Sonawane, Avinash Kumar Agarwal*

Engine Research Laboratory, Department of Mechanical Engineering

Indian Institute of Technology Kanpur, Kanpur-208016, India

*Corresponding Author's email: akag@iitk.ac.in

Supporting Information

S1. Combustion Characteristics at Different Engine Speeds

Figure S1(a) shows the effect of engine speed on the in-cylinder pressure variation of the engine fueled with different gasohol vis-à-vis baseline gasoline at a fixed engine torque of 30 Nm. At lower engine speed (1500 rpm), flame velocity was relatively lower due to a lack of turbulence in the combustion chamber, leading to a relatively slower heat release. This resulted in two peaks in the in-cylinder pressure curve corresponding to motoring (without combustion) and combustion, respectively. Turbulence in the engine combustion chamber increased with increasing engine speed, which improved fuel-air mixing, leading to faster combustion and heat release. This could also be seen in the P-θ curves, where P_{max} increased with increasing engine speed up to medium engine speed (2500 rpm). At higher engine speed (3500 rpm), less time available for fuel-air mixing, especially in GM10 and GE10, led to relatively lower P_{max}. Higher latent heat of vaporization and the presence of moisture traces might be the reasons for the slower chemical kinetics of gasohol-air mixtures. Figure S1(a) showed that the P_{max} of gasohol was relatively higher than gasoline. Improved combustion due to contributions of fuel oxygen present in gasohol was the main reason for this trend, which was dominant up to medium engine speeds. However, other fuel properties such as latent heat of vaporization (in GM10) and moisture content (in GE10) became more dominant at higher engine speeds, leading to relatively lower P_{max} [S1]. Relatively higher research octane number (RON) of alcohols than gasoline resulted in quicker heat release and pressure rise without knocking. The slightly different combustion behavior of GB10 was another important observation of this study. Relatively lower in-cylinder charge cooling effect of GB10 resulted in higher P_{max} compared to other test fuels. GM10 exhibited second-highest P_{max} due to the combined effect of higher flame speed and oxygen content of methanol [S2].

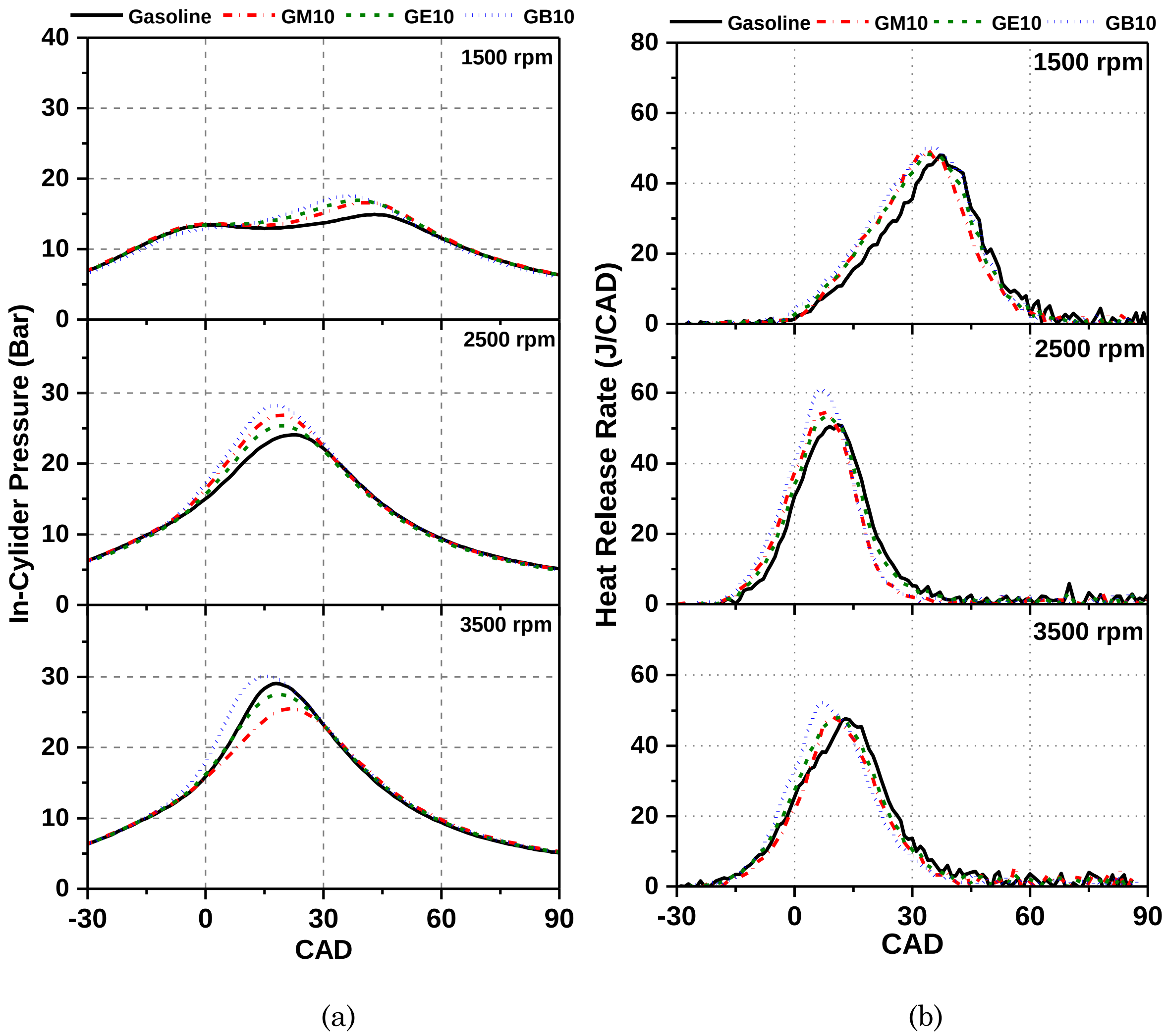

Figure S1: (a) In-cylinder pressure and (b) heat release rate variations w.r.t. crank angle position at different engine speeds at 30 Nm

Figure S1(b) shows that HRR_{max} increased with increasing engine speed from 1500 rpm to 2500 rpm. However, a further increase in engine speed resulted in relatively lower HRR_{max}. Due to increased turbulence at higher engine speeds, dominant heat transfer might be a possible reason for relatively lower HRR_{max}. The effect of improved fuel-air mixing was also visible in the HRR trends, which showed relatively advanced HRR_{max} at 2500 rpm. However, the HRR curve exhibited a slightly retarded peak at 3500 rpm. At low engine speed, gasohol exhibited a similar HRR pattern with the same HRR_{max} as gasoline. GB10 exhibited relatively superior combustion at higher engine speeds compared to gasohol, and HRR trends of GM10 and GE10 were almost similar. HRR_{max} of all gasohol was slightly shifted toward the bTDC compared to gasoline. Relatively higher flame speed of alcohol present in gasohol was the main reason for this behavior, resulting in relatively quicker heat release and faster combustion than gasoline.

Figure S2 showed SoC, CP, and CD variations of gasoline and gasohol-fueled engine at varying engine speeds and at a constant engine load of 30 Nm. Results showed that SoC advanced with increasing engine speed up to 2500 rpm and remained constant at higher engine speeds. At higher engine speeds, SoC advanced mainly due to increased turbulence and in-cylinder temperature, which resulted in faster fuel-air combustion kinetics. Higher turbulence in the combustion chamber improved the charge formation and shortened the physical ignition delay. At higher speeds, increased fuel quantity in the fuel-air mixture also affected the combustion kinetics and advanced SOC up to medium engine loads (30 Nm). Higher engine loads, dominant in-cylinder cooling effects of test fuels reduced the fuel-air chemical kinetics, leading to slightly retarded SoC of all test fuels. Results show that gasohol resulted in relatively advanced SoC compared to gasoline. Among different gasohol, GB10 exhibited the most advanced SoC. However, GM10 exhibited the most retarded SoC. The relatively higher reactivity of butanol and higher latent heat of vaporization were the responsible factors for the SoC trends of GB10 and GM10, respectively. The differences between SoC of test fuels at different engine speeds were relatively lower than SoC's differences at various engine loads. This was an important observation, which shows that fuel-air chemical kinetics was more sensitive to engine load.

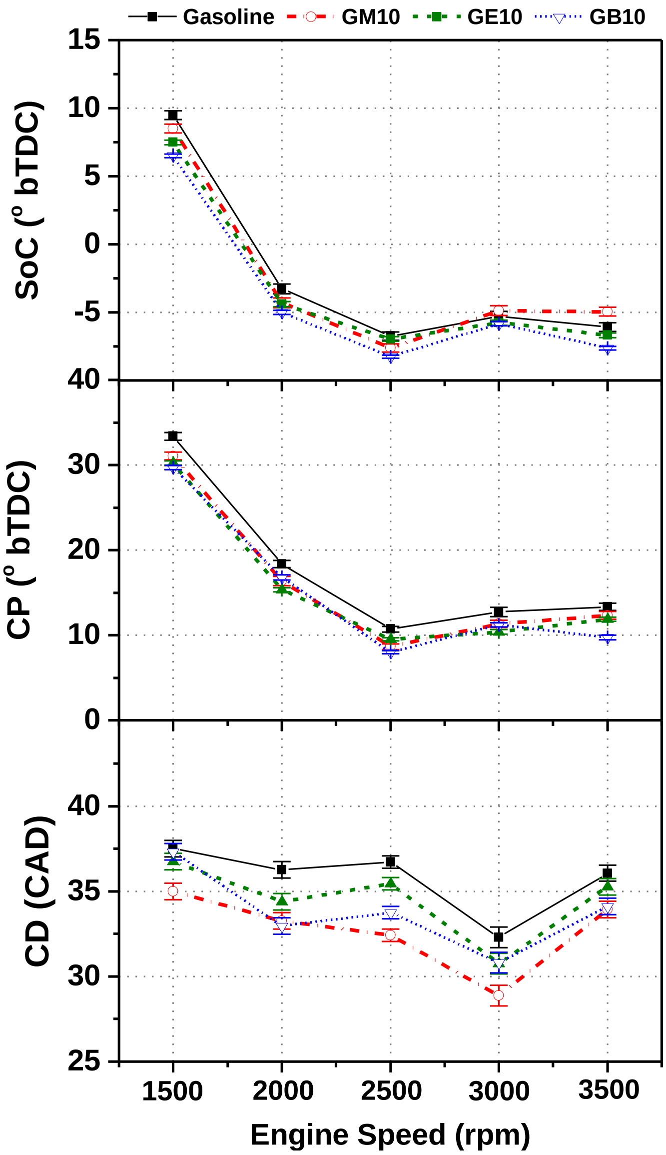

Figure S2: SoC, CP, and CD at different engine speeds at 30 Nm

Figure S2 shows that CP has followed a similar trend as that of SoC at different engine speeds. For all test fuels, CP advanced with increasing engine speed. Relatively faster fuel-air chemical kinetics due to higher in-cylinder temperature and higher flame speed due to increased turbulence were the main reasons for this trend. Relatively advanced CP of gasohol compared to baseline gasoline was another important observation. Relatively higher flame speed of alcohol than baseline gasoline was the main reason for these trends, resulting in more rapid combustion. Among different gasohol, GB10 exhibited relatively advanced CP compared to other test fuels. However, the difference between CP of all gasohol was insignificant (except at 3500 rpm). CD trends showed a slightly random pattern at different engine loads, which decreased up to 3000 rpm and then suddenly increased at 3500 rpm. This might be due to the relative dominance between heat loss and turbulence. At 3500 rpm, more heat loss due to both increased in-cylinder temperature and turbulence resulted in more CD compared to other lower engine speeds. At all engine speeds, gasohol exhibited a relatively shorter CD compared to baseline gasoline. Relatively superior combustion due to the higher flame speed of alcohol and fuel-bound oxygen were the important factors responsible for this trend. Among different gasohol, GM20 exhibited the shortest CD followed by GB10. This was mainly due to faster flame propagation and fuel-air chemical kinetics of GM10 and GB10, respectively. GM 10 shows the shortest CD due to the higher flame velocity and reactivity nature of methanol.

S2. Performance Characteristics at Different Engine Speeds

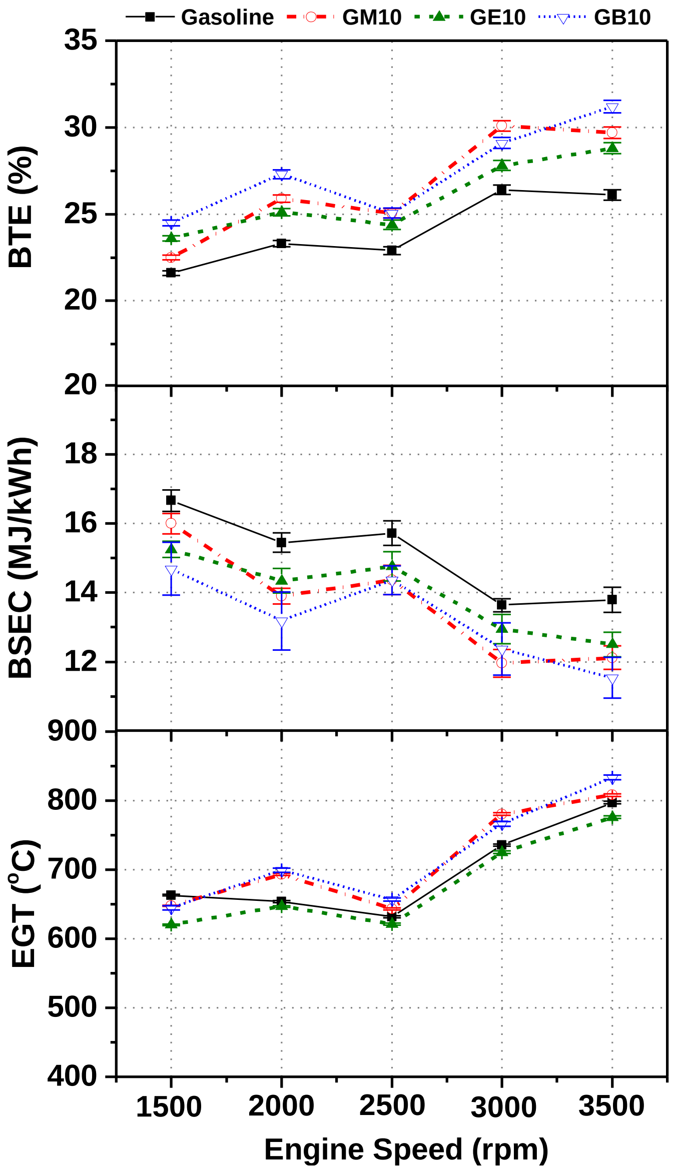

Figure S3: BTE, BSEC, and EGT at different engine speeds and 30 Nm

In the figure, S3 shows that the BTE variation at different engine speeds flowed a random pattern, increasing and decreasing up to 2500 rpm, and then exhibited a sudden increase at 3000 rpm. Increasing engine speed resulted in more turbulence, which affects both heat loss from cylinder walls and flame velocity. BTE variations at different engine speeds were mainly due to the relative dominance of increased heat loss and increased flame velocity at higher engine speeds. Reduced volumetric efficiency at higher engine speeds might be another important factor for relatively lower constant BTE at too high an engine speed (3500 rpm). Gasohol showed relatively higher BTE compared to baseline gasoline. Higher volumetric efficiency of the gasohol-fueled engine due to charge cooling effect, the higher flame velocity of gasohol, and the presence of fuel-bound oxygen might be the possible reasons for better performance of gasohol compared to gasoline. Among different gasohol, GB10 exhibited the highest BTE, followed by GM10. Relatively more reactivity of butanol and higher flame speed of methanol were the main reasons for the higher BTE of GB10 and GM10, respectively. Among different gasohol, GE10 exhibited the lowest BTE. The presence of moisture traces might be the possible reason for this. BSEC followed a random decreasing trend with increasing engine speed.

Gasohol exhibited relatively lower BSEC compared to baseline gasoline. Among different test fuels, the BSEC of the GB10-fuelled engine was lowest at most of the engine speeds (except 3000 rpm). Similar to other performance parameters, EGT also followed a randomly increasing pattern with increasing engine speed. Results show that the EGT of GM10 and GB10 first increased (up to 2000 rpm) and then decreased upon a further increase in speed (up to 2500 rpm). However, the EGTs of GE10 and baseline gasoline was almost constant up to 2500 rpm. After 2500 rpm, EGTs of all test fuels increased drastically and reached up to ~800°C at 3500 rpm. At lower engine speeds (up to 2500 rpm), the relative dominance of heat transfer and increased in-cylinder temperature might be responsible for this trend. However, at higher engine speeds, a dominant increase in in-cylinder temperature due to more fuel quantity and less time available for heat transfer might be the important reasons for higher EGT. Among different test fuels, GM10 and GB10 exhibited relatively higher EGT compared to GE10 and baseline gasoline. Improved combustion characteristics of these test fuels were the main reason for this trend [S3]. At all engine speeds, GE10 exhibited the lowest EGT due to the small content of moisture traces in ethanol, which absorbed a fraction of combustion energy, leading to inferior engine performance and lower EGT. Overall, figure S3 shows that all performance parameters exhibited a trade-off between governing parameters such as in-cylinder temperature, heat transfer, flame speed, charge cooling effect, volumetric efficiency at ~2500 rpm.

S3. Emission Characteristics at Different Engine Speeds

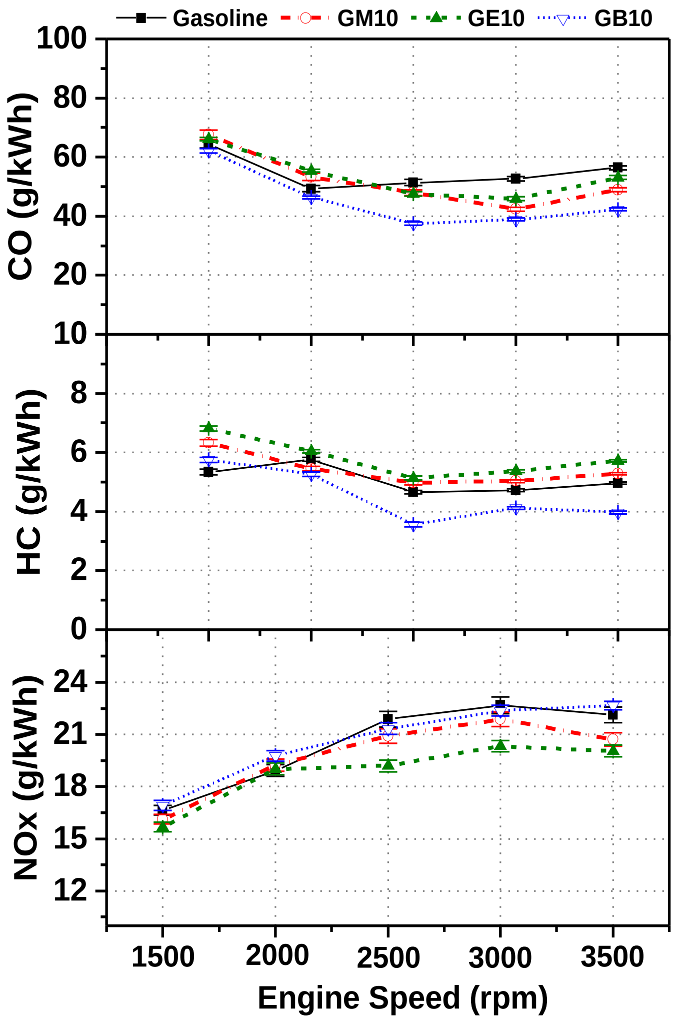

Figure S4: CO, HC, and NOx emitted at different engine speeds and 30 Nm

Figure S4 shows regulated emission characteristics of gasohol and gasoline-fueled engine at engine speeds and at constant engine load (30 Nm). Results show that CO emission decreased slightly up to medium engine speed and then exhibited a slight increase at higher engine speeds. With increasing engine speed, increasing in-cylinder temperature promoted CO-to-CO_2 oxidation, leading to lower CO emission. However, at too high engine speed, increased heat loss due to higher peak in-cylinder temperature and more turbulence reduced the bulk in-cylinder temperature, which promoted the CO emission. At higher engine speed, relatively lesser time available to complete the CO-to-CO_2 conversion might be another responsible factor for higher CO emission. The effect of fuel-bound oxygen in gasohol was visible in CO emissions trends, which exhibited the gasohol emitted relatively lower CO than baseline gasoline. At lower engine speed, slightly higher CO emissions from GM10 and GE10-fuelled engines might be attributed to methanol and ethanol's dominant charge cooling effect. GB10 emitted relatively lower CO compared to GM10 and GE10. Advanced SoC and CP of GB10 were the main reason for this behavior, ensuring complete combustion. HC emissions trends of different test fuels at different engine speeds followed similar CO emissions, which slightly reduced with increasing engine speed.

At lower engine speed, HC emissions were slightly higher due to the too lean fuel-air mixture, which led to incomplete combustion in the presence of lower in-cylinder temperature. With increasing engine speed, increased in-cylinder temperature promoted faster fuel-air chemical kinetics, and higher turbulence increased the flame speed, leading to complete combustion of fuel. This resulted in slightly lower HC emissions at higher engine speeds; however, at too high engine speed, a trade-off between increased heat transfer due to turbulence and increased in-cylinder temperature due to more fuel quantity led to insignificant variation in HC emissions at higher engine speed. Figure S4 shows that GM10 and GE10 emitted relatively higher HC emissions than baseline gasoline; however, HC emissions from the GB10-fuelled engine were relatively lower than baseline gasoline. More charge cooling of GM10 and GE10 due to higher latent heat of vaporization of methanol and ethanol might be the possible reason for this trend, which resulted in lower in-cylinder temperature, leading to incomplete combustion. The higher reactivity of butanol and lower latent heat of vaporization promoted the combustion of GB10, leading to relatively lower HC emissions compared to other test fuels. Figure S4 shows that NOx emissions increased with increasing engine speed; however, at higher engine speeds, NOx emission remained constant. The increased in-cylinder temperature at higher engine speeds might be the possible reason for higher NOx emissions; however, increased turbulence at too high engine speed led to excessive heat loss from the cylinder walls, which resulted in lower NOx formation. The lesser time available to complete the NOx formation reactions at higher engine speeds might be another reason for insignificant variation in NOx emissions at higher engine speed. At higher engine speeds, all gasohol emitted relatively lower NOx compared to baseline gasoline. However, at lower engine speeds, NOx emissions from the GB10-fuelled engine were slightly higher than baseline gasoline. The dominant charge cooling effect of alcohols compared to gasoline might be the main reason for lower NOx emissions from gasohol, especially at higher speeds. Relatively slower fuel-air chemical kinetics also affected the NOx formation mechanism, leading to lesser NOx formation. The effect of in-cylinder cooling due to the presence of moisture traces in GE10 was visible in NOx trends of GE10, which emitted the lowest NOx at all engine speeds.

S4. Unregulated Emission Characteristics at different Engine Speeds

S4.1 Emission of oxides of nitrogen, sulfur dioxide, and ammonia

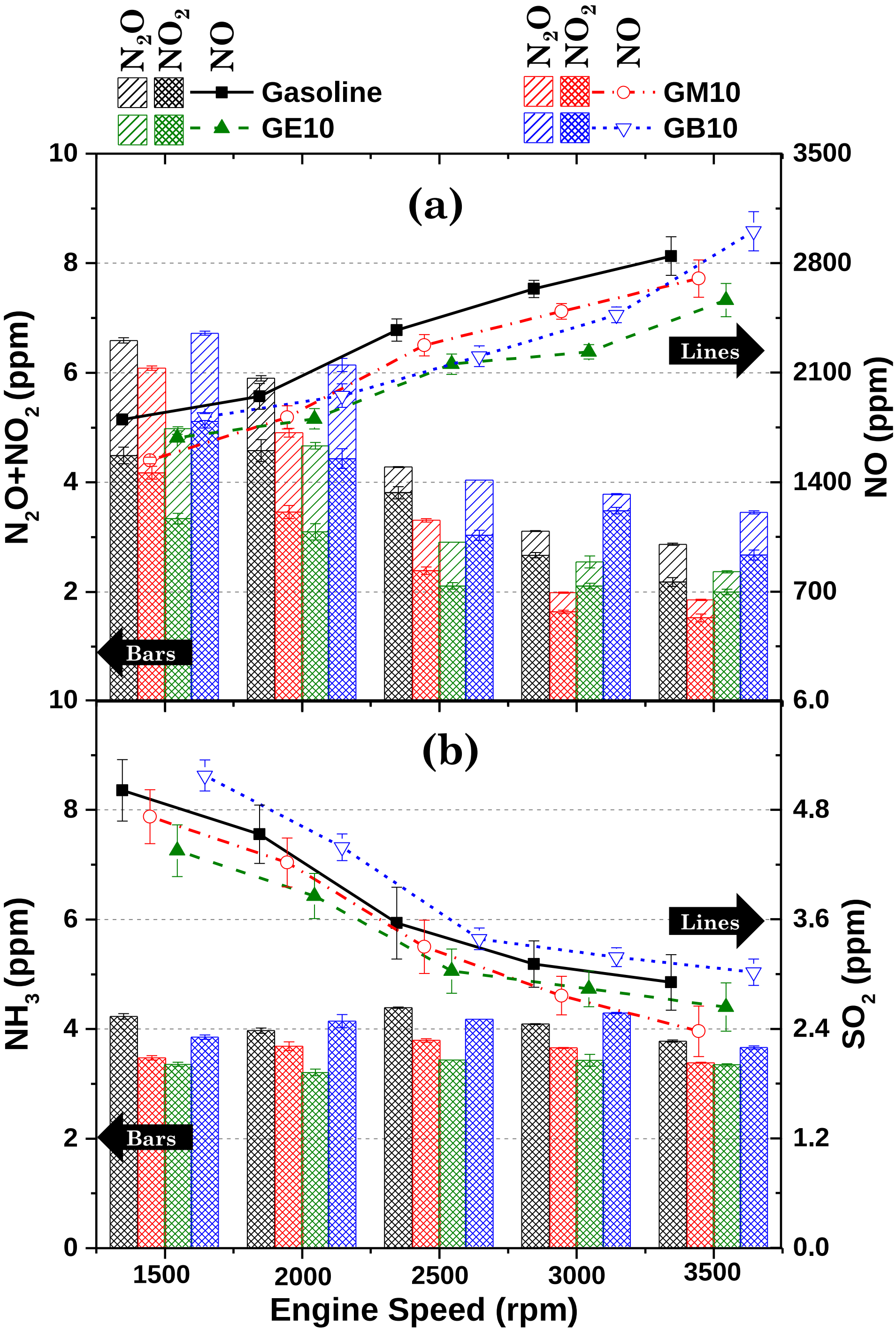

Figure S5: (a) Oxides of nitrogen, (b) sulfur dioxide, and ammonia emitted t different engine speeds and 30 Nm

Figure S5(a) shows the variation in nitrogen oxides with an engine speed for gasohol and gasoline-fueled engine at 30 Nm. NO emission increased with an increase in engine speed due to a rise in peak in-cylinder temperature [S4]. Gasohol-fueled engine emitted a relatively lower NO compared to baseline gasoline. Relatively lower in-cylinder temperature due to more cooling effects caused by alcohol might be possible for this trend. GE10 showed the lowest NO emission at higher engine speed among different gasohol due to the presence of small moisture content in ethanol, which reduced peak in-cylinder temperature. GM10 emitted relatively lower NO emission at low engine speed due to higher latent heat of vaporization of methanol compared to other alcohols. NO concentrations were significant for all test fuel and contributed to a major portion of NOx. For all test fuels, NO_2 Emission is reduced with increasing engine speed.

Gasohol exhibited relatively lower NO_2 emissions compared to baseline gasoline. For all test fuels, N_2O Emission is reduced with increasing engine speed. The availability of less oxygen at higher engine speed might be the possible reason for this trend. Gasoline shows lower N_2O emissions compared to gasohol due to more oxygen deficiency. Figure S5(b) shows the variation of SO_2 and NH_3 emitted from gasoline and gasohol-fueled engine at different engine speeds and at constant engine load (30 Nm). For all test fuels, SO_2 decreased with an increase in engine speed. This might be mainly due to improved combustion at higher engine speeds. Similar to engine load variation, the gasohol-fueled engine emitted relatively lower SO_2 compared to baseline gasoline. However, the difference between the concentrations of SO_2 from different test fuels was not significant. Among different gasohol, GE10 showed the lowest SO_2 Emission. NH_3 Emission was observed to be almost constant with variation in engine speed. Gasohol showed lower NH_3 Emission compared to gasoline at all engine speed. Amongst all gasohol, GE10 exhibited the lowest NH_3 Emission at all engine speed.

S4.2 Emissions of formaldehyde, formic acid, and isocyanic acid

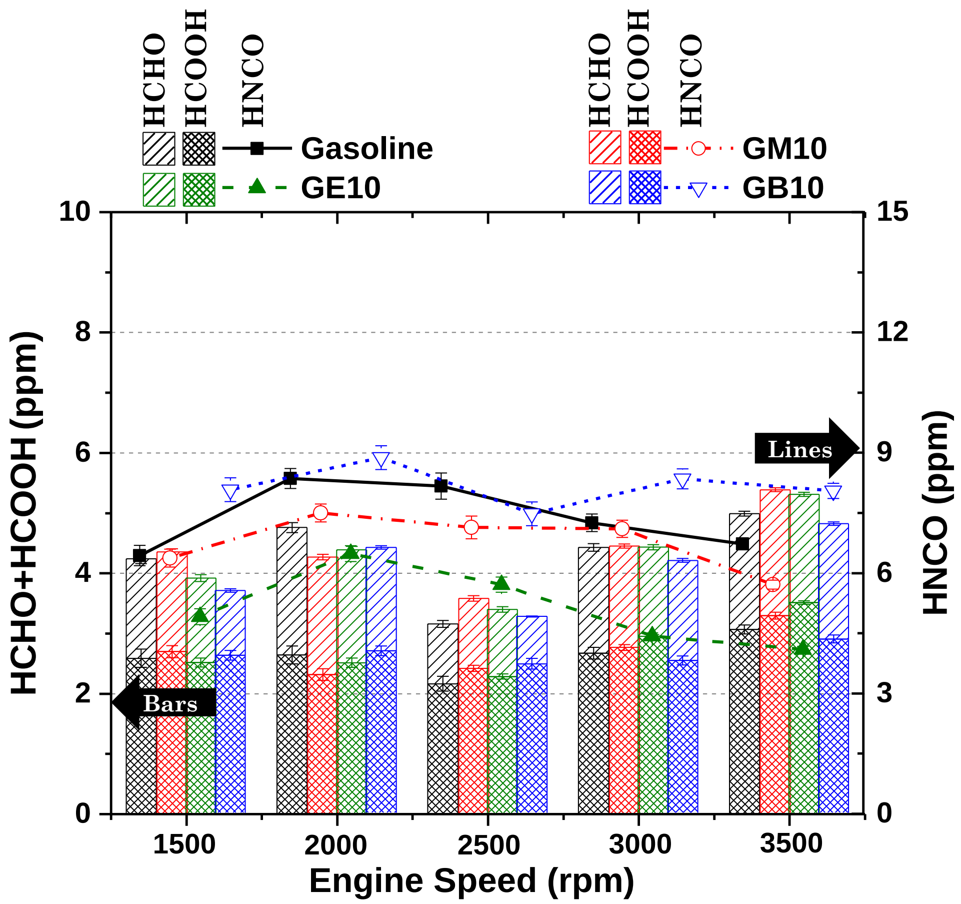

Figure S6: Formaldehyde, formic acid, and isocyanic acid emitted at different engine speeds and 30 Nm

Figure S6 shows the variation of HCHO, HCOOH, and HNCO emitted from gasoline and gasohol-fueled engine at different engine speeds and at constant engine load (30Nm). The result shows that as engine speed increased, HCHO emission reduced slightly and then increased with further increasing engine speed. The increased in-cylinder temperature at higher engine speeds was the main reason for lower HCHO emissions. However, a further increase in engine speed led to incomplete combustion of the fuel-air mixture due to less time available to complete the reactions and less oxygen availability. This resulted in more incomplete combustion products such as HCHO and HCOOH at higher engine speeds. Above 2500 rpm, increased turbulence inside the combustion chamber promoted heat losses to the surrounding, leading to lower in-cylinder temperature and higher HCHO emission. Gasohol shows a comparable HCHO emission at lower engine speeds, which increased at higher engine speeds. At higher engine speeds, the presence of inherent oxygen led to superior combustion, leading to lesser HCHO formation for the GB10-fuelled engine; however, the dominant charge cooling effect of methanol and ethanol hampered the completeness of reaction, leading to more HCHO emission at higher engine speed. Among different gasohol, GE10 exhibited the highest HCHO emission at higher engine speed. HCOOH emission has a random trend in engine speed variation, and the difference between HCCO emissions from gasohol and the gasoline-fueled engine was also not significant. The effect of higher in-cylinder temperature was visible in HCHO emissions, which exhibited that GB 10 has the lowest HCOOH emission. For all test fuels, HNCO emission was almost constant at different engine speeds. Among different test fuels, GE10 showed the lowest HNCO emission, followed by GM10. This clearly shows the dominant effect of in-cylinder temperature (EGT) on HNCO formation.

S4.3 Emission of unsaturated and aromatic hydrocarbons

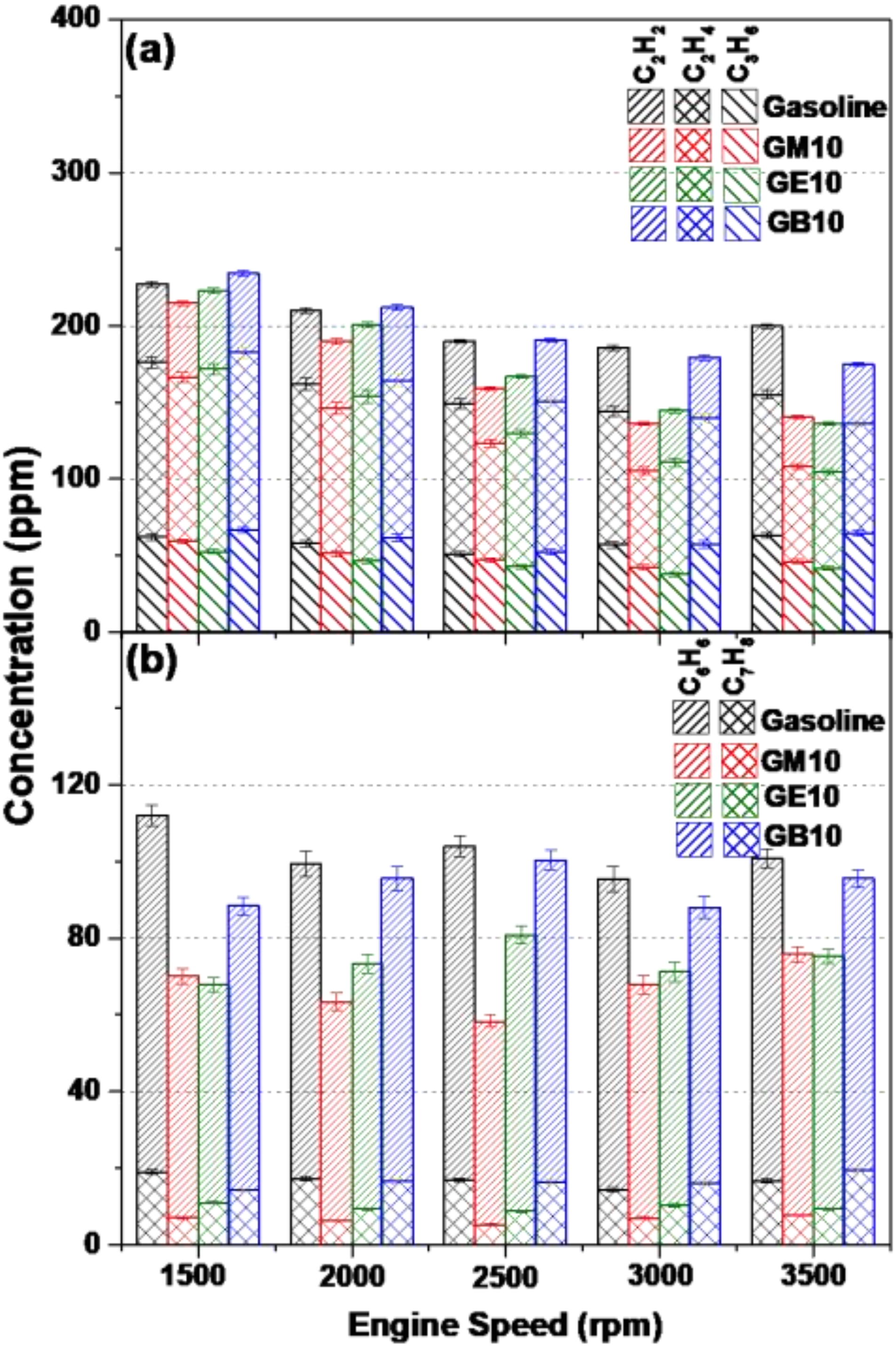

Figure S7: (a) Unsaturated and (b) aromatic hydrocarbons emitted at different engine speeds and 30 Nm

Figure S7(a) shows the concentration of unsaturated hydrocarbons emitted from gasoline and gasohol-fueled engine at different engine speeds and at constant engine load (30 Nm). Results show that the Emission of unsaturated hydrocarbons (C_2H_2, C_2H_4, and C_3H_6) reduced with an increased engine speed for all test fuels. Relatively superior combustion due to more turbulence and increased in-cylinder at higher engine speed were the main reasons for lower Emissions of C_2H_2, C_2H_4, and C_3H_6 at higher engine speeds. In addition, the presence of higher in-cylinder temperature promoted the oxidation of intermediate combustion products, leading to lower emissions of C_2H_2, C_2H_4, and C_3H_6. Among different test fuels, GM10 and GE10 emitted relatively lower C_2H_2, C_2H_4, and C_3H_6 compared to gasoline. However, unsaturated hydrocarbons emitted from GB10-fuelled engines were almost equivalent to baseline gasoline. The presence of oxygen might be another factor responsible for these trends, which promoted the oxidation of these unsaturated hydrocarbons. Figure S7(b) showed the variation of aromatic species emitted from gasoline and gasohol-fueled engine at different engine speeds and at constant engine load (30Nm). Results show that C_6H_6 Emission was almost constant with variation in engine speed for all test fuel. At all engine speeds, gasohol exhibited relatively lower benzene emissions compared to gasoline. Among different gasohol, GM10 exhibited the lowest benzene emission, followed by GE10. The concentration of benzene emitted from GB10 was almost similar to that of gasoline. These trends show that benzene formation was dominantly affected by inherent oxygen present in the test fuels. C7H8 Emission exhibited a similar trend for all test fuels as C_6H_6 Emission with a variation of engine speed.

References

[S1] Aghahossein, S.S., Abdollahipoor, B., Windom, B., Reardon, K.F., Foust, T.D. Effects of blending C3-C4 alcohols on motor gasoline properties and performance of spark ignition engines: A review. Fuel Processing Technology 2020; 197: 106194.

[S2] Gong, C., Li, Z., Chen, Y., Liu, J., Liu, F., Han. Y. Influence of ignition timing on combustion and emissions of a spark-ignition methanol engine with added hydrogen under lean-burn conditions. Fuel 2019; 235:227–38.

[S3] Prasad, B.S.N., Kumar G.N. Influence of ignition timing on performance and emission characteristics of an SI engine fueled with an equal-volume blend of methanol and gasoline. Energy Sources, Part A: Recovery, Utilization, and Environmental Effects 2019; 1-15.

[S4] Heywood, J.B. Internal combustion engine fundamentals. New York: McGraw-Hill; 1988.